

Towards water-insensitive CO₂-binding organic liquids for CO₂ absorption: Effect of amines as promoter

Ali Hedayati, Farzaneh Feyzi *

Thermodynamics Research Laboratory, School of Chemical Engineering, Iran University of Science and Technology, Tehran 1684613114, Iran



ARTICLE INFO

Article history:

Received 19 December 2019

Received in revised form 25 February 2020

Accepted 18 March 2020

Available online 19 March 2020

Keywords:

CO₂ capture

Switchable ionic liquids

Switchable solvents

Mixture design approach

CO₂-binding organic liquids

ABSTRACT

CO₂-binding organic liquids (CO₂-BOLs) or reversible ionic liquids (RILs), are non-aqueous CO₂-triggered switchable polarity solvents which can be used for energy efficient CO₂ capture. In this study, the novel three-component CO₂-BOLs are introduced. They are comprised of 1,8-Diazabicyclo[5.4.0]undec-7-ene (DBU) as an organic superbase and an alkanol in conjunction with an amine as a promoter. Screening experiments were performed to find the best combination of CO₂-BOL components based on CO₂ loading and absorption rate. The variables were: the type of alcohol (methanol, n-butanol, sec-butanol, tert-butanol and 1-hexanol) and the type of amine (EEA, MEA, AMP, DEA, AEEA, PZ, TETA and DETA) using the DBU superbase. Statistical mixture design approach using Minitab 18 software was implemented for the design of experiments, modeling and optimization of CO₂ loading at the fixed temperature of 35 °C and the initial CO₂ pressure of 25 bar. It was found that DBU/MeOH/MEA system with the molar ratio of 0.3/0.17/0.53 has the maximum equilibrium absorption (α_{eq}) and CO₂ uptake within 30 min (α_R) of 0.444 and 0.267 mol CO₂/mol solvent, respectively. Amine additives promoted absorption efficiency and inhibited formation of solid precipitates (bicarbonate salt) in the presence of water impurity. Characterization of ionic species and explaining the water-inhibitory effect of MEA were obtained from FTIR, ¹H NMR and ¹³C NMR spectroscopic analysis. Equilibrium CO₂ solubility data in DBU/MeOH (1/2) and DBU/MeOH/MEA (0.3/0.6/0.1) CO₂-BOLs were also obtained at temperatures of 308.2 and 318.2 K and pressure range of 0–33 bar. The results of present study can be used to effectively utilize CO₂-BOLs in the wet conditions with higher absorption efficiency and lower regeneration energy.

© 2020 Elsevier B.V. All rights reserved.

1. Introduction

The environment is suffering from profound changes, like global warming, which result in severe challenges to human survival and development [1,2]. The immense amounts of CO₂ emission into the atmosphere (~30 Gt/year), as a greenhouse gas, is the major contributor to climate change [3,4]. Therefore, there is an urgent need to employ efficient CO₂ capture techniques to attain a significant decrease in anthropogenic CO₂ production from pre-combustion and post-combustion sources [5]. Moreover, CO₂ is an acidic gas with destructive effects such as corrosion in equipment and poisoning of catalysts in process industries [6]. CO₂ can be considered as a precious source of carbon due to the possible usage of CO₂ conversion, representing the importance of new CO₂ sorbents development [7].

Currently, the chemical absorption of CO₂ is conventionally performed via aqueous solutions of alkanolamines, including monoethanolamine (MEA), diethanolamine (DEA) and *N*-methyl-diethanolamine (MDEA) at

relatively low temperatures that results in the production of carbamate and bicarbonate salts [8].

Amine-based technologies have serious intrinsic disadvantages such as: high energy consumption in solvent regeneration at 393–403 K due to heat capacity and vaporization enthalpy of water, solvent evaporation during process, equipment corrosion, relatively low CO₂ uptake of 0.5 mol CO₂/mol amine, requirement for solvent dilution due to the corrosive nature of amines and solvent degradation during the process [9–11].

Such drawbacks have led researchers to develop new effective solvent systems [12]. Non-aqueous solvents, that replace water with organic solvents, were investigated for CO₂ capture. Zhuang and Clements [13] investigated CO₂ absorption into the biphasic liquid absorbents consisting of MEA and methylaminoethanol (MAE) in isoctanol and 1-heptanol, respectively, by implementing a batch-mode apparatus. Kim et al. [14] used the phase transitional alkanolamine–alcohol mixtures for CO₂ absorption. They showed that these solvents had economic advantages over aqueous-amine solutions due to the lower regeneration energies. Barzaghi et al. [15] studied the CO₂ uptake by alkanolamines in aqueous and 2-(2-methoxyethoxy)ethanol (DEGMME) solutions. It was found that aqueous alkanolamine solutions had higher CO₂ loading values, while non-

* Corresponding author.

E-mail addresses: ali_hedayati@chemeng.iust.ac.ir (A. Hedayati), feyzi@iust.ac.ir (F. Feyzi).

aqueous solutions had higher absorption rates. Non-aqueous MEA [16,17], 2-(2-aminoethyl)amine (AEEA) [18], 2-amino-2-methyl-1-propanol (AMP) [19–21], Triethanolamine (TEA) [22], tertiary amines [23], DEA and diisopropanolamine (DIPA) [24] were also evaluated for CO₂ capture.

Moreover, conventional (i.e. non-switchable) ionic liquids (ILs) have attracted the attention of scientists for CO₂ capture due to their advantages including tunability of structure, high thermal and chemical stability, negligible vapor pressure and high selectivity [25,26]. Nevertheless, the disadvantages of ILs such as: high viscosity, complicated synthetic process, high cost and toxicity limit their usability in industrial applications [27,28].

Recently, a novel class of green non-aqueous solvents called CO₂-binding organic liquids (CO₂-BOLs) or switchable ionic liquids (SILs) have been investigated for CO₂ capture [29]. SILs are switchable polarity solvents (SPSs) based on Jessop's "switchable solvents" that utilize CO₂ as a chemical trigger to transform between non-ionic and ionic liquid forms [30,31]. The most common SILs are comprised of an alcohol and a non-nucleophilic organic base (amidine or guanidine) which chemically bind CO₂ to form alkylcarbonate salts [32,33]. Some of the advantages of SILs over other liquid solvents are as follows [34–37]:

- Reversible binding of CO₂.
- No requirement for inert solvents due to the liquid state of SILs after CO₂ absorption leading to the higher loading.
- CO₂ absorption of SILs (19 wt% by 1,8-diazabicyclo-[5.4.0]-undec-7-ene (DBU):1-hexanol) being significantly higher than aqueous MEA solvents (<7 wt% by 30% aqueous MEA).
- Combination of chemical and physical absorption of CO₂.
- Low energy consumption for solvent regeneration. CO₂ binds more weakly in alkylcarbonate salts relative to carbamate and bicarbonate salts (products of aqueous-amine solvents) due to the decreased hydrogen bonding. Also, the SILs have lower heat capacities than aqueous amine solutions. The reaction could be reverted by heating below the solvent (SIL) boiling point or even by bubbling an inert gas, like nitrogen at low temperatures (323 K).
- Designability of SILs the like conventional ionic liquids by altering or modifying the components.
- Production of SILs from cheaper precursors in comparison with aprotic ionic liquids.
- Lower alkalinity of alcohol-based solvents than aqueous amines.
- Reduced solvent loss by choosing the low vapor pressure components in SILs.
- The possibility of solvent recovery and recycling using their switching properties (change in polarity) [27].

Two-component BOLs comprised of an alcohol and DBU have been used as a solvent for CO₂ capture. Hellebrant et al. [34] investigated CO₂ absorption in a mixture of DBU and organic alcohols including 1-hexanol, 1-pentanol, 1-butanol, 1-propanol and 2-propanol. Among investigated solvents, DBU/1-butanol system had the highest CO₂ absorption rate of 0.88 (mol CO₂/mol DBU) in acetonitrile at 25 °C and 1 atm. Wang et al. [38] evaluated the CO₂ absorption capacity of an equimolar mixture of DBU and alcohol-functionalized ionic liquids at 20 °C and atmospheric pressure. The CO₂ loadings of DBU/[Im₂OH][Tf₂N] and DBU/[N_{ip,21}OH][Tf₂N] mixtures were determined to be 1.04 and 1.02 mol CO₂/mol DBU, respectively. Privalova et al. [9] compared the performance of CO₂ removal using classical ILs and SILs. They used DBU as superbase in conjunction with 1-hexanol and different amino-alcohols including 4-amino-1-butanol, 6-amino-1-hexanol and L-prolinol. On average, CO₂ loading using SILs was more than ten times higher than physical ILs and >0.3 M higher than acetate-based ILs. The highest absorption capacity was obtained to be 1.07 mol CO₂/mol ROH using 6-amino-1-hexanol as alcohol at atmospheric pressure and 22 °C. Carrera et al. [11] studied solvent systems based on saccharides (D-Mannose, D-

Glucose, β-Cyclodextrin, Alginic Acid and Mannitol) in conjunction with DBU for CO₂ capture. They obtained the highest loading of 13.9 wt% using D-mannose: DBU (ratio eq. = 0.625) system where 3.3/5 of alcohol groups converted to carbonates. Cao et al. [39] used an equimolar mixture of methanol and DBU at 1 atm and room temperature which resulted in the absorption of 0.74 mol CO₂/mol DBU, while Xie et al. [31] achieved the theoretical ratio of 1:1:1 using CO₂ protective atmosphere and surplus methanol. Ozturk et al. [40] investigated the kinetics of CO₂ absorption in the CO₂-BOLs comprised of DBU (2.5–10 wt%) and alkanol (1-hexanol and 1-propanol). The calculated activation energies were much lower than conventional solvents for CO₂ which leads to energy saving during CO₂ desorption process. Also, the reaction rate constants and reaction orders were comparable with industrial aqueous solvents. Whyatt et al. [41] studied the CO₂ absorption behavior in CO₂BOLs using a wetted-wall contactor. It was found that the physical solubility of CO₂ in CO₂BOLs is higher than that of aqueous amines. CO₂ solubility in DBU-glycerol solutions with different proportions at temperatures from 302 to 353 K was measured and modeled by Ostonen et al. [42].

However, the main drawback of superbase/alcohol CO₂-BOLs for CO₂ capture is that it must be prepared, handled and used under scrupulously dry conditions. Existence of trace amounts of water in the reaction environment leads to the production and precipitation of solid bicarbonate salt that restricts its performance for industrial applications and increases the regeneration energies [43].

Chiral ionic liquids derived from amidines/amino-acid esters/CO₂ [44], amidines/aliphatic primary amines/CO₂ [45] and amidines/chiral amino alcohols/CO₂ [46] were observed to be water resistant such that the addition of water up to 10 wt% did not impede the formation of ionic liquids upon exposure to CO₂. However, amidinium carbamates were derived in the mentioned systems which are more stable than carbonate salt that results in higher regeneration temperature.

Consequently, in this study novel water tolerable CO₂-BOL solvents were produced by addition of primary and secondary amines as promoters to mixtures of DBU and different alcohols. The present study is aimed at screening of 8 different primary, secondary and polyamines including: MEA, N-ethylethanolamine (EEA), Diethanolamine (DEA), AEEA, piperazine (PZ), AMP, Triethylenetetramine (TETA) and Diethylenetriamine (DETA), 5 alcohols including: methanol, 1-butanol, sec-butanol, tert-butanol and 1-hexanol based on the CO₂ absorption rate and equilibrium solubility of CO₂. Screening experiments were implemented as an effective way to find the potential absorber before further characterization. A mixture design approach was used to optimize the molar fraction of ternary system components (amine, superbase and alcohol) to attain maximum equilibrium CO₂ uptake and absorption rate. The selected BOL systems were further characterized to investigate the production of ionic species and explain the water-inhibitory effect of the added promoter to the two-component CO₂-BOL of DBU and alkanol.

2. Materials and methods

2.1. Chemicals

Methanol (purity ≥99.9%), n-butanol (purity ≥99.5%), sec-butanol (purity ≥99.0%), tert-butanol (purity ≥99.5%), 1-hexanol (purity ≥98.0%), DBU (purity ≥98.0%), EEA (purity ≥97.0%), MEA (purity ≥99.0%), AMP (purity ≥95.0%), DEA (purity ≥99.0%), AEEA (purity ≥98.0%), PZ (purity ≥99.0%), TETA (mixture of isomers, purity ≥95.0%) and DETA (purity ≥98.0%) were all purchase from Merck. The chemicals were distilled and dried over a molecular sieve such that the water contents were found to be <20 ppm using the Karl Fischer titration method (Metrohm, 831 KF Coulometer). High purity CO₂ from Roham Gas Co. (purity >99.9%) was used as-received condition in the absorption experiments. The chemical structures of the base and tested amines are reported in Table 1.

Table 1

Name, acronym and chemical structure of the base and amines in this study.

Name	Acronym	Molecular structure
1,8-Diazabicyclo(5.4.0)undec-7-ene	DBU	
Ethanolamine	MEA	
N-ethylethanamine	EEA	
diethanolamine	DEA	
2-(2-Aminoethyl)ethanol	AEEA	
Diethylenetriamine	DETA	
Triethylenetetramine	TETA	
Piperazine	PZ	
2-Amino-2-methyl-1-propanol	AMP	

2.2. CO₂ absorption: apparatus and procedure

Fig. 1 shows the CO₂ solubility measurement equipment in this study schematically. This setup consists of: (1) CO₂ cylinder, (2) gas container (stainless steel with volume of 182 ml), (3) autoclave reactor (stainless steel, total volume = 37 ml, diameter = 2.5 cm, height = 5.5 cm, pipeline volume = 10 ml) with a circulating water jacket, (4) magnetic stirrer (Fisher, Cat. No. 14-511-113-113), (5) circulating water bath (LAUDA Alpha RA 8, 248–373 K) and (6) data acquisition system (ADAM-4019+ and computer). The gas container and autoclave were equipped with pressure sensors (PS₁ and PS₂) (Sensys, Model: M5156-11700X-050BG×-050BG with the accuracy of ±2.5 kPa) and temperature sensors (TS₁ and TS₂) (K-type with the accuracy of ±0.1 K).

The CO₂ absorption rate and equilibrium solubility data which were used in screening experiments and mixture design method were obtained via the following procedure:

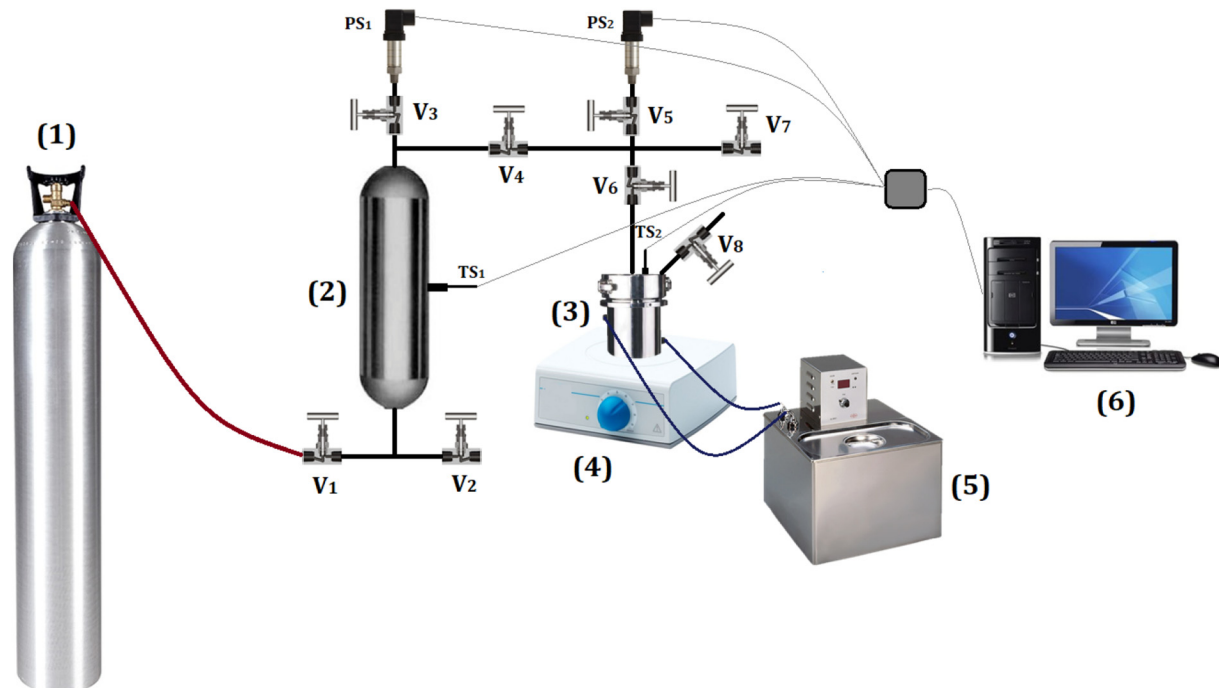


Fig. 1. Schematic of the experimental setup for CO₂ absorption; (1) CO₂ cylinder, (2) gas container, (3) autoclave reactor, (4) magnetic stirrer, (5) circulating water bath and (6) computer.

- 1- The autoclave and gas container were evacuated to 0.01 bar (Heraeus vacuum pump, ID. No: 76-0-53237) through valve V_7 .
- 2- Valve V_4 was closed and the solvent was charged into the autoclave from valve V_8 . The total amount of solvent was kept constant at 0.045 mol in all the experiments.
- 3- The gas container was filled up to the pressure of 30.10 bar at ambient temperature through valve V_1 .
- 4- The autoclave temperature was set to 308.2 K in all the experiments using a water circulating bath.
- 5- The absorption process was started by opening valve V_4 (while valves V_7 and V_8 were closed) which exerts the initial pressure of 25.00 bar to the autoclave and then valve V_4 was closed to record the pressure decrease versus time for 30 min. It should be noted that the mixer was switched off to measure the molecular diffusion into the solvent during the experiments.
- 6- Equilibrium solubility data at the initial pressure of 25.00 bar, the temperature of 308.2 K and the predetermined type and concentration of solvent was obtained by turning the stirrer on and recording the pressure profile until reaching the equilibrium state.
- 7- The CO_2 loading (α) data were obtained by the proposed method of Park and Sandall [47] which has been used in previous publications [48–50]:

The amount of injected CO_2 into the reaction vessel from the gas container was obtained as follows:

$$n_{\text{CO}_2} = \frac{V_{\text{gc}}}{R} \left(\frac{P_1}{Z_1 T_1} - \frac{P_2}{Z_2 T_2} \right) \quad (1)$$

Z , R , V_{gc} , P and T are the compressibility factor, the universal gas constant, the volume, the pressure and the temperature of gas container, respectively. Subscripts 1 and 2 refer to the conditions before and after CO_2 injection, respectively.

The equilibrium pressure of CO_2 (P_{CO_2}) was obtained from:

$$P_{\text{CO}_2} = P_t - P_s^* \quad (2)$$

P_t and P_s^* are the total pressure and the vapor pressure of solvent (SIL), respectively. The number of moles of unabsorbed CO_2 in the gas phase ($n_{\text{CO}_2}^g$) was obtained as follows:

$$n_{\text{CO}_2}^g = \frac{V_g P_{\text{CO}_2}}{Z_{\text{CO}_2} RT} \quad (3)$$

V_g is the gas phase volume in the autoclave and was calculated from Eq. (4). The Peng-Robinson equation of state [51] was used for calculation of compressibility factors in the gas phase.

$$V_g = V - V_s \quad (4)$$

V is the volume of the autoclave and V_s is the volume of the injected solvent into the autoclave.

The number of moles of absorbed CO_2 into the solvent ($n_{\text{CO}_2}^l$) was calculated by Eq. (5):

$$n_{\text{CO}_2}^l = n_{\text{CO}_2} - n_{\text{CO}_2}^g \quad (5)$$

Finally, CO_2 loading in the solvent was obtained by the following equations:

$$\alpha_{\text{eq}} = \frac{\text{number of absorbed CO}_2 \text{ molecules at equilibrium}}{n_{\text{solvent}}} \quad (6)$$

$$\alpha_R = \frac{\text{number of absorbed CO}_2 \text{ molecules within 30 min}}{n_{\text{solvent}}} \quad (7)$$

where n_{solvent} was defined as the total number of moles of solvent (i.e. $n_{\text{alcohol}} + n_{\text{amine}} + n_{\text{base}}$).

2.3. Characterization

The synthesized ionic compounds were characterized and the presence of ionic products was proved employing nuclear magnetic resonance spectroscopy (NMR) using Brucker's Avance 500-MHz instrument. The NMR spectra of samples were referenced to CDCl_3 as an internal standard. All the NMR spectra were processed using SpinWorks 4 processing software. Fourier-transform infrared spectroscopy (FTIR) was also used for characterization and analyzing the functional groups of BOLs before and after CO_2 absorption using Shimadzu-8400S instrument. The production of ionic species in the reaction medium was evidenced by FTIR spectroscopy.

3. Results and discussion

3.1. Validation experiments

Before the experiments using SILs, the authenticity of equipment, measurements and calculations were validated. Accordingly, the equilibrium solubility data of CO_2 in aqueous solutions containing 2.9 and 7.0 mol MEA/kg H_2O were compared with the results of Wagner et al. [52] at two different temperatures of 313.2 and 353.2 K. Results are reported in Table 2. The average absolute deviation (AAD), maximum deviation and minimum deviation between the data in this work and literature were found to be 2.04%, −5.22% and −0.22%, respectively; which indicates good agreement with the published data.

3.2. Screening experiment

Screening experiments were conducted to determine the best combination of base, alcohol and amine in three-component CO_2 -BOLs. The experiments were designed to specify the most appropriate solvent based on CO_2 absorption rate and equilibrium absorption of CO_2 . Accordingly, the amine type (MEA, EEA, DEA, AEEA, DETA, TETA, PZ and AMP) was changed while the superbase (DBU) and alcohol (1-hexanol) were fixed. Then, the selected amine was used as a promoter in the DBU base solvents where different alcohols (methanol, n-butanol, sec-butanol, tert-butanol and 1-hexanol) were implemented for CO_2 absorption. The mole fractions of components were kept constant in all the experiments at 0.3, 0.1 and 0.6 for DBU, amine and alcohol, respectively. The absorption temperature and initial CO_2 pressure were chosen to be 308.2 K and 25.00 bar.

The profiles of CO_2 absorption in the DBU/1-hexanol CO_2 -BOLs versus time using eight different amine additives are illustrated in Fig. 2-a. Moreover, the CO_2 uptake of BOLs was calculated up to the equilibrium condition (α_{eq}) where no sensible pressure change was observed in the reactor (Fig. 2-b). Accordingly, the performance of amine additives for CO_2 loading within 30 min (α_R) and α_{eq} were in the following orders:

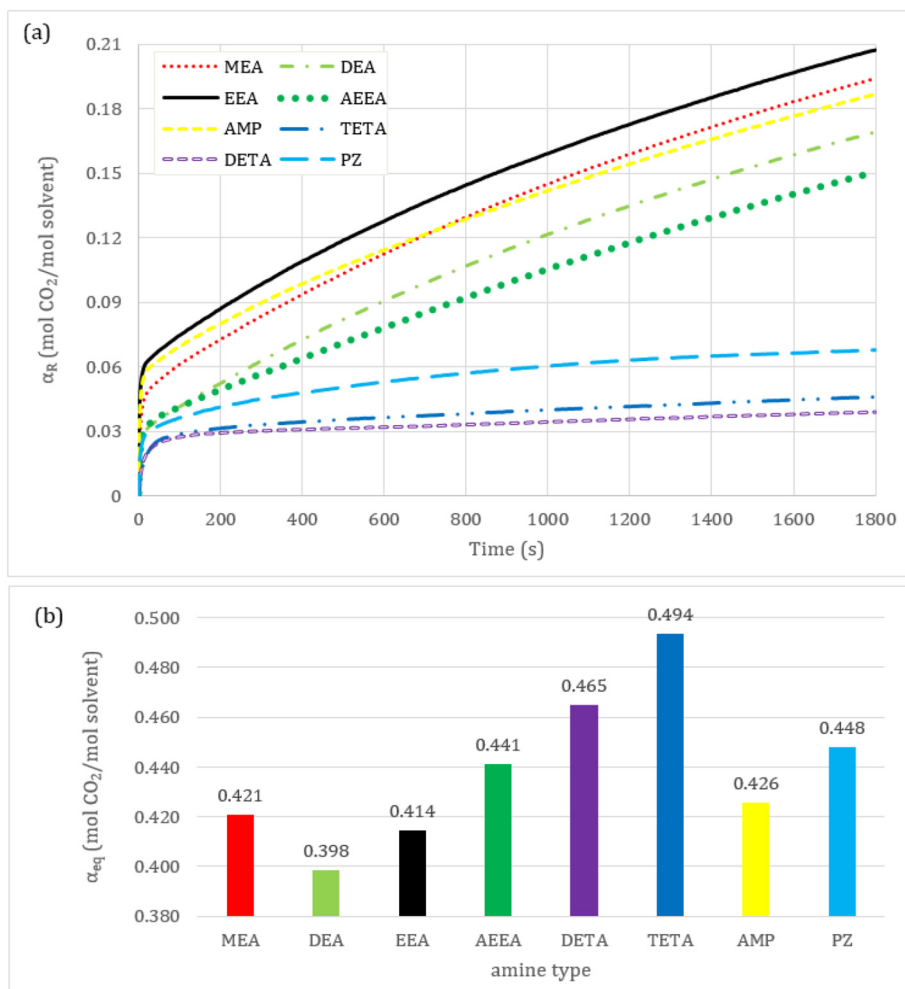
$$\begin{aligned} \alpha_R: &\text{EEA} > \text{MEA} > \text{AMP} > \text{DEA} > \text{AEEA} > \text{PZ} > \text{TETA} > \text{DETA}. \\ \alpha_{\text{eq}}: &\text{TETA} > \text{DETA} > \text{PZ} > \text{AEEA} > \text{AMP} > \text{MEA} > \text{EEA} > \text{DEA}. \end{aligned}$$

The CO_2 absorption properties can be influenced by the existence of various functional groups, the number of amine groups, the presence of a cyclic structure and steric hindrance that are identified to affect the amine basicity [53,54]. However, in this study the amine can serve simultaneously as an alcohol in the DBU/amine/ CO_2 reaction and as a base in amine/alcohol/ CO_2 reaction [34], which can complicate the explanation of the role of amine.

It was observed that increasing the number of amine functional groups in amine additives enhances the equilibrium CO_2 absorption of BOLs. The maximum and minimum equilibrium CO_2 uptakes were obtained to be 0.494 and 0.398 mol CO_2 /mol solvent using TETA and DEA as a promoter, respectively.

Table 2Comparison between the experimental CO₂ solubility data in aqueous MEA solutions in this work and literature data [52].

T [K]	The concentration of aqueous MEA solution [mol MEA/kg H ₂ O]	P _t [bar]	$\alpha_{CO_2}^a$ (this work)	α_{CO_2} (literature) [52]	R.D. [%] ^b
313.2	2.9	2.78	0.745	0.750	-0.666
		10.41	0.916	0.900	1.777
		14.80	0.968	0.954	1.467
		20.24	1.030	1.009	2.081
		24.78	1.077	1.047	2.865
		30.01	1.099	1.087	1.103
313.2	7	2.90	0.641	0.667	-3.898
		11.09	0.779	0.803	-2.988
		18.75	0.858	0.863	-0.579
		23.45	0.887	0.889	-0.224
		28.90	0.919	0.914	0.547
		35.32	0.949	0.939	1.064
353.2	7	1.23	0.472	0.498	-5.220
		6.10	0.581	0.605	-3.966
		11.13	0.633	0.649	-2.465
		17.03	0.659	0.686	-3.935
		24.69	0.725	0.723	0.276
		29.65	0.754	0.742	1.617
AAD (%) ^c = 2.041					

^a α_{CO_2} =(mol of CO₂ per mol of amine).^b Relative deviation (%)= $\frac{\alpha_{exp}-\alpha_{lit}}{\alpha_{lit}} \times 100$ ^c Average absolute deviation (%)= $\frac{1}{N} \sum_{i=1}^N \frac{|\alpha_{exp,i}-\alpha_{lit,i}|}{\alpha_{lit,i}} \times 100$.**Fig. 2.** Effect of amine on the (a) CO₂ loading versus reaction time and (b) equilibrium CO₂ absorption from the initial pressure of 25.00 bar at the constant temperature of 308.2 K using DBU/1-hexanol/amine (0.3/0.6/0.1) CO₂-BOL.

The CO_2 absorption rate using various amines can be attributed to the physicochemical properties of solvents, including diffusivity and solubility of CO_2 in the liquid medium, and kinetics of the reaction [55,56]. Among tested amines, EEA had the highest α_R of 0.207 mol CO_2 /mol solvent. In this regard, the more unsatisfactory performance was obtained by PZ, TETA and DETA mainly due to the formation of highly viscous, cloudy and even solid products which inhibited the diffusion of CO_2 into the absorber. It was observed that the amines without hydroxyl group (PZ, DETA and TETA) resulted in the formation of solid products, forming a carbamate salt rather than an alkylcarbonate salt. Therefore, despite the best performance for equilibrium CO_2 absorption, the reduced absorption rate and production of solid ionic products limited their applicability.

Comparing α_R and α_{eq} of the amine promoted solvents resulted in the selection of MEA for the alcohol screening experiments. Although, EEA promoted system had the highest α_R , MEA is a cheaper source and exhibited a better α_{eq} . Moreover, the lower molecular weight of MEA leads to the higher weight capacity of MEA compared to EEA promoted system.

Fig. 3 illustrates the effect of alcohol (methanol, 1-hexanol, n-butanol, sec-butanol and tert-butanol) in the three-component BOLs comprised of DBU, alcohol and amine (0.3/0.6/0.1) at the fixed temperature of 308.2 K and the initial reactor pressure of 25.00 bar. Generally, the rate constant of reaction reflects the solvent effect. It has been shown that the solubility parameter of a solvent has a linear relation with the reaction rate constant in organic solvents [57]. Accordingly, among the evaluated alcohols, methanol had the highest absorption rate equal to 0.252 mol CO_2 /mol solvent.

Comparing the equilibrium CO_2 loading by BOLs using different alcohols revealed that the choice of alcohol had no significant influence on CO_2 absorption capacity ($\alpha_{eq} = 0.417\text{--}0.425$). But, the chain length of alcohols changes the physical properties (e.g. viscosity and melting point) of BOLs to make them molecularly tunable [58]. The polarity of BOLs is also related to the alcohol chain length such that higher differences in polarity between ionic and neutral forms can be achieved using shorter alcohols [59]. Hellebrant et al. [34] concluded that the values of ΔG and ΔH of reactions using different alcohols in the two-component BOLs were almost independent of the choice of alcohol.

3.3. Mixture design models

Mixture design approach was used to evaluate the effect of component proportions in the three-component SILs (DBU/MEA/MeOH). Statistical mixture design is one of the most powerful approaches for the design of experiments (DOEs) [60] which have been used extensively in various fields such as chemistry [61], chemical engineering [62], material science [63], biochemistry [64], food engineering [65] and environmental science [66]. Mixture design is a special class of response surface methodology (RSM) that is used for modeling and optimization of response variables based on the proportions of the components (independent variables). Implementation of this technique reduces the costs of experiments by preventing waste of materials and time, and illuminates the influence of mixture components and their interactions on the dependent variables.

In this study extreme vertex design (design degree = 3) with 3 components was chosen for modeling of the three-component BOL. Extreme

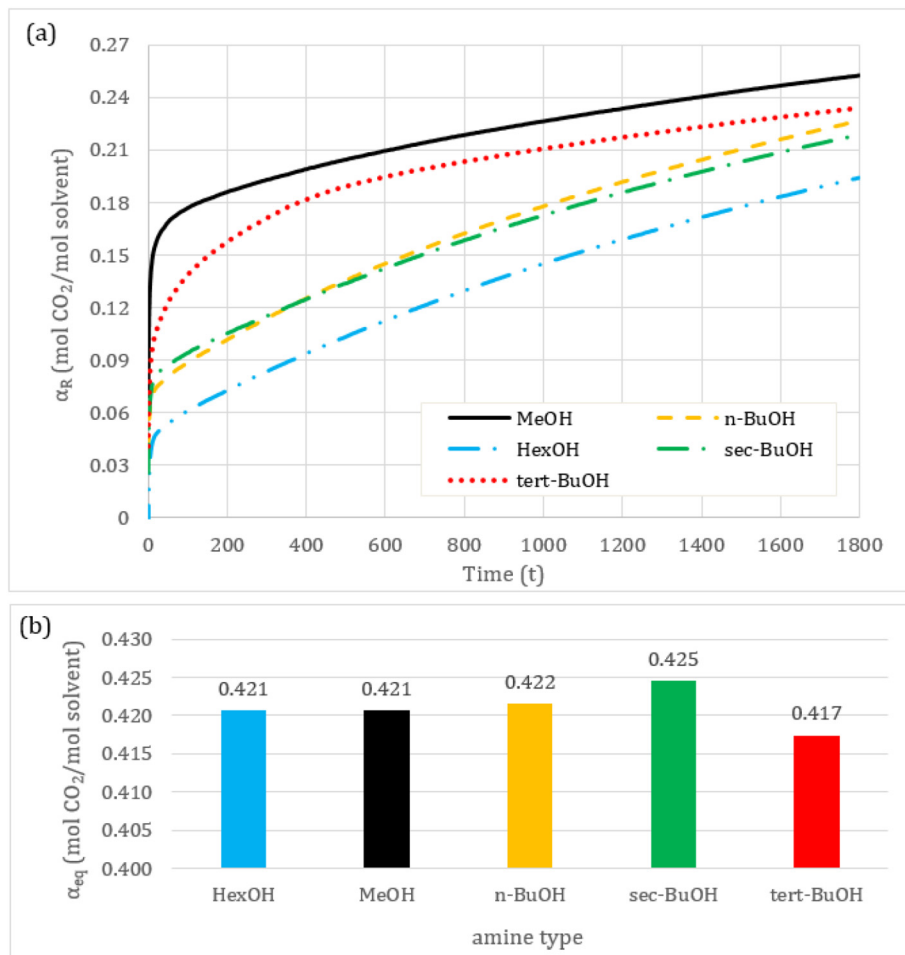


Fig. 3. Effect of alcohol on the (a) CO_2 loading versus reaction time and (b) equilibrium CO_2 absorption from the initial pressure of 25.00 bar at the constant temperature of 308.2 K using DBU/alcohol/MEA (0.3/0.6/0.1) CO_2 -BOL.

vertex design was used due to the constraints on the components mole fraction: $0.1 < \text{DBU} < 0.5$, $0.3 < \text{MeOH} < 0.9$ and $0 < \text{MEA} < 0.2$. The responses in mixture design were calculated by Eqs. (6) and (7):

The experimental data for α_{eq} and α_R were fitted by the special cubic model (Eq. (8)) and are further discussed in Section 3.3.1.

$$Y = \sum_{i=1}^q \beta_i Z_i + \sum_{i \neq j}^q \beta_{ij} Z_i Z_j + \sum_{i \neq j \neq k}^q \beta_{ijk} Z_i Z_j Z_k \quad (9)$$

Y , Z_i , β_i and q are the estimated response, molar fraction of the i th component in the solvent mixture, the coefficient of model and the number of components in the mixture, respectively.

3.3.1. Evaluation of mixture design models for CO_2 absorption

The responses of designed experiments in Table 3 were used to calculate the coefficients of the special cubic equation (Eq. (9)) by the statistical mixture design approach. The positions of designed experiments in the triangular contour plots are specified in Fig. 4. Tables 4 and 5 show the regression coefficients and the analysis of variance (ANOVA) for the proposed models of α_R and α_{eq} .

The p-values in these tables determine the significance of each term statistically. Model terms with $p < .001$, $0.001 \leq p < .05$ and $p \geq .05$ were considered as highly significant, significant and insignificant, respectively.

Based on these criteria, the fitted models for α_R and α_{eq} were verified ($p = .000$) via ANOVA. In the obtained model for α_R , all the linear terms and the quadratic term of $A \times B$ were highly significant ($p < .001$) while other model terms were significant ($0.001 \leq p < .05$). In the case of α_{eq} , all model terms except the quadratic interaction term of alcohol and base ($A \times B$) were insignificant.

Eqs. (9) and (10) present the models for α_R ($R^2 = 98.13\%$ and adj- $R^2 = 96.26\%$) and α_{eq} ($R^2 = 98.45\%$ and adj- $R^2 = 96.90\%$) as a function of components mole fraction, respectively.

$$\begin{aligned} \alpha_R = & 0.0318A - 1.3047B - 1.569C + 3.0155AB + 3.058AC \\ & + 7.72BC - 9.71ABC \end{aligned} \quad (10)$$

$$\begin{aligned} \alpha_{eq} = & 0.07846A - 0.086B + 0.17C + 1.590AB + 0.34AC + 1.57BC \\ & + 1.33ABC \end{aligned} \quad (11)$$

3.3.2. Effect of mole fraction of components

Fig. 4 shows the effect of components (DBU, MEA and MeOH) mole fraction on the α_{eq} and α_R at the fixed temperature of 308.2 K and the initial pressure of 25.00 bar. Cox response trace plots (Fig. 5) also provide more information about the effects of components on the α_R and α_{eq} :

- As the mole fraction of DBU in the mixture increases from 0.10 (DBU/MEA/MeOH = 0.1/0.128/0.772) to 0.50 (DBU/MEA/MeOH = 0.5/0.071/0.429) at the fixed proportion of MeOH to MEA of 6, α_{eq} increases from 0.265 to 0.429 mol CO_2 /mol solvent. Higher amount of superbase in the solvent results in the production of more ionic species which has a positive effect on equilibrium CO_2 absorption. However, addition of DBU to the solvent has the opposite effect on α_R . On one hand, increasing DBU mole fraction from 0.10 to the optimum value of 0.25 (DBU/MEA/MeOH = 0.25/0.107/0.643) results in a higher absorption rate, on the other hand, more DBU mole fraction beyond 0.25 has a negative effect on α_R , probably due to the increased viscosity of BOL.
- Higher amounts of MeOH over the entire range of mole fraction of components decreases the equilibrium CO_2 absorption due to lower superbase or amine in the reaction medium. Increasing the MeOH mole fraction up to the optimum composition of (DBU/MeOH/MEA = 0.257/0.657/0.086) results in the maximum α_R of 0.286 mol CO_2 /mol solvent due to the decreased viscosity and enhanced CO_2 diffusivity in the liquid medium. However, more MeOH concentration lowers the absorption rate of solvent.
- Addition of MEA has the opposite effects on the solvent performance. Increasing MEA concentration from 0 in the binary mixture of DBU/MeOH (0.33/0.67) to 0.2 (DBU/MEA/MeOH = 0.27/0.2/0.53) results in the enhancement of α_{eq} from 0.375 to 0.437 mol CO_2 /mol solvent, but reduces α_R from 0.287 to 0.265 mol CO_2 /mol solvent due to the higher solvent viscosity.

3.3.3. Determination of optimum operation conditions

The proposed models for α_R (Eq. (9)) and α_{eq} (Eq. (10)) were used to determine the optimum solvent composition. Accordingly, the maximum α_{eq} of 0.444 mol CO_2 /mol solvent and the maximum α_R of 0.267 mol CO_2 /mol solvent were achieved at DBU, MEA and MeOH

Table 3
Designed experiments by mixture design approach and the observed responses for α_R and α_{eq} .

Run Order	MeOH (A)	DBU (B)	MEA (C)	α_{eq} (experiment)	α_{eq} (model)	α_R (experiment)	α_R (model)
1	0.45	0.40	0.15	0.460	0.470	0.225	0.232
	0.75	0.20	0.05	0.317	0.334	0.270	0.277
2	0.50	0.30	0.20	0.472	0.459	0.268	0.262
	0.55	0.40	0.05	0.421	0.427	0.244	0.243
4	0.65	0.20	0.15	0.348	0.378	0.269	0.275
	0.50	0.50	0.00	0.390	0.398	0.145	0.152
6	0.90	0.10	0.00	0.200	0.213	0.182	0.182
	0.70	0.30	0.00	0.372	0.369	0.302	0.293
8	0.70	0.10	0.20	0.285	0.296	0.248	0.245
	0.30	0.50	0.20	0.465	0.473	0.178	0.181
10	0.40	0.50	0.10	0.449	0.446	0.160	0.149
	0.80	0.10	0.10	0.272	0.259	0.237	0.235
12	0.60	0.30	0.10	0.418	0.421	0.280	0.279
	13						

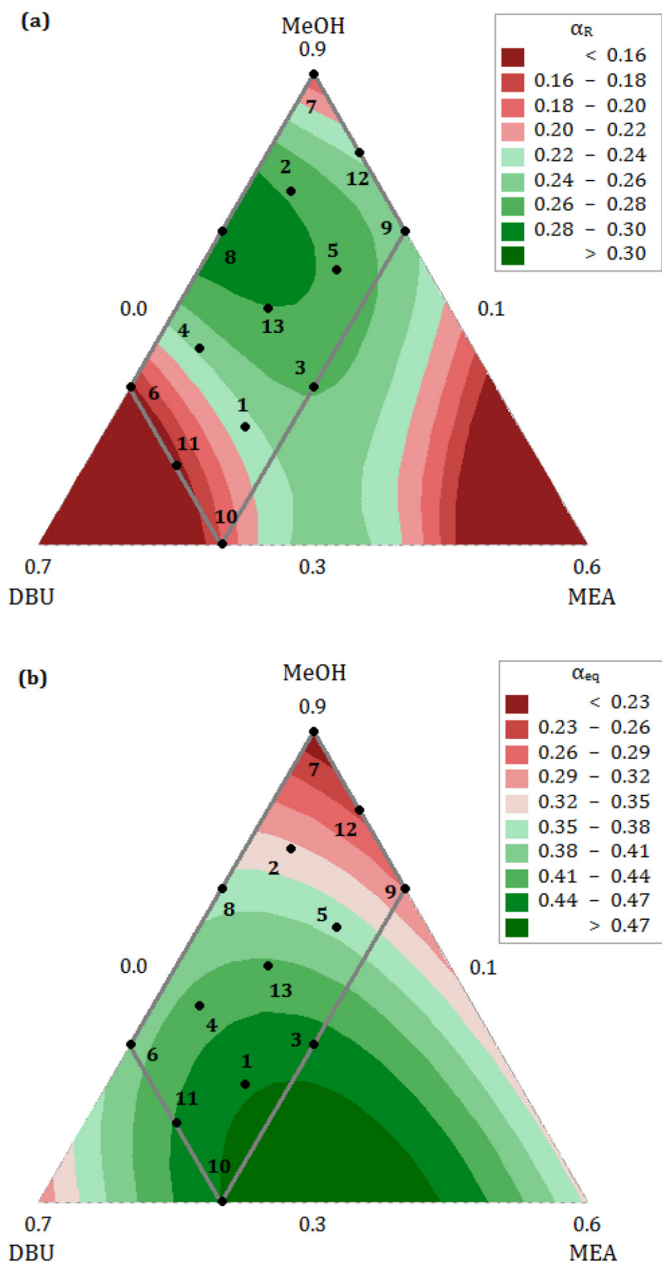


Fig. 4. Contour plots for the effect of components proportions on the (a) α_R and (b) α_{eq} in the DBU/MEA/MeOH BOL at the initial pressure of 25.00 bar and the temperature of 308.2 K.

mole fraction of 0.3, 0.17 and 0.53, respectively. The optimal point was validated by triplicate experiments which resulted in the α_R and α_{eq} of 0.44 ± 0.02 and 0.26 ± 0.01 mol CO₂/mol solvent, respectively.

3.4. DBU/MEA/MeOH ternary system

Addition of MEA to DBU/MeOH CO₂-BOL not only has a positive effect on the CO₂ absorption loading but also leads to the inhibition of solid products formation even in the presence of water in reaction medium. In order to investigate the effect of MEA as an additive in the two-component CO₂-BOLs, the FTIR, ¹H NMR and ¹³C NMR spectroscopy was performed on the two-component CO₂-BOLs of DBU/MeOH and DBU/MEA as well as on the DBU/MeOH/MEA as a three-component CO₂-BOL before and after reaction with CO₂. Moreover, the reaction products were further analyzed by NMR spectroscopy after addition of water as impurity to the DBU/MeOH, DBU/MEA and DBU/MeOH/MEA BOLs. The employed solvents in characterization experiments were equimolar mixtures of components, while the mole fraction of water was chosen to be 0.3 in the wet solvents. Finally, a plausible reaction mechanism is proposed to explain the effect of MEA on the formed ionic species in the reaction mixture.

3.4.1. Nuclear magnetic resonance (NMR) spectroscopy

3.4.1.1. DBU/MeOH and DBU/MEA systems. NMR spectra were collected to characterize DBU/MeOH and DBU/MEA mixtures as well as the ionic product of DBU/MeOH/CO₂ reaction ($[DBUH^+][CH_3OCOO^-]$) based on Path1 of Fig. 6 and the ionic product of DBU/MEA/CO₂ reaction ($[DBUH^+][MEACOO^-]$) based on Path2 of Fig. 6.

The products of DBU/MeOH/CO₂ and DBU/MEA/CO₂ appeared to be a viscous clear liquid and a white solid, respectively. The ¹H and ¹³C NMR spectroscopy was used to confirm the formation of ionic products. The ¹H NMR spectra of DBU/MeOH, DBU/MeOH/CO₂, DBU/MEA and DBU/MEA/CO₂ are shown in Fig. 7. Table 6 shows the chemical shifts assignment in the ¹H NMR spectroscopy. The attributed atom numbers of DBU, MeOH and MEA molecules and the ionic product are shown in Fig. 7. The broad peak at 6.08 ppm for the product of CO₂ reaction with DBU/MeOH BOL belongs to the N—H proton of DBU (C_{8'}) which supports the formation of $[DBUH^+][MeOCO_2^-]$.

The ¹H NMR spectrum of $[DBUH^+][MEACOO^-]$ shows that the signals deshielded in comparison with unreacted DBU/MEA mixture. The largest change in the chemical shifts is observed to be for the protons at position 6 in DBU (0.34 ppm) and at position a (0.39 ppm) in MEA. The protonation of DBU at position 8 (N—H) was confirmed by the appearance of a new peak at 4.49 ppm in the ¹H NMR spectrum of ionic product ($[DBUH^+][MEACOO^-]$).

Further, the formation of ionic compounds is also supported by ¹³C NMR spectroscopic studies (Table 7). The ¹³C NMR spectrum of DBU/MeOH mixture after reaction with CO₂ (Fig. 8-b) represents a new carbon signal at $\delta = 158.34$ ppm that was attributed to the carbonyl carbon of methylcarbonate anion (CH₃COO⁻). Furthermore, the peak of carbon

Table 4
Regression coefficients and analysis of variance (ANOVA) for the predicted special-cubic model of α_R

Source	DF	Coef.	SE Coef.	Seq SS	Adj SS	Adj MS	F-value	T-value	p-Value
Regression	6			0.029426	0.029426	0.004904	63.50		0.000
Linear	2			0.007252	0.018903	0.009451	122.37		0.000
A		0.0318	0.0182						
B		-1.3047	0.0988						
C		-1.569	0.546						
Quadratic	3			0.019380	0.020269	0.006756	87.47		0.000
A × B	1	3.155	0.215	0.015701	0.016612	0.016612	215.08	14.67	0.000
A × C	1	3.058	0.747	0.002903	0.001295	0.001295	16.76	4.09	0.006
B × C	1	7.72	1.14	0.000776	0.003553	0.003553	46.00	6.78	0.001
Special cubic	1			0.002794	0.002794	0.002794	36.17		0.001
A × B × C	1	-9.71	1.61	0.002794	0.002794	0.002794	36.17	-6.01	0.001
Residual error	6			0.000463	0.000463	0.000077			
Total	12			0.029890					

Table 5

Regression coefficients and analysis of variance (ANOVA) for the predicted special-cubic model of α_{eq}

Source	DF	Coef.	SE Coef.	Seq SS	Adj SS	Adj MS	F-value	T-value	p-Value
Regression	6			0.086025	0.086025	0.014338	52.45		0.000
Linear	2	0.0784	0.0342	0.073567	0.000325	0.000163	0.59		0.581
A		-0.086	0.186						
B		0.17	1.03						
Quadratic	3			0.012407	0.008144	0.002715	9.93		0.010
A × B	1	1.590	0.405	0.008978	0.004218	0.004218	15.43	3.93	0.008
A × C	1	0.34	1.41	0.002223	0.000016	0.000016	0.06	0.24	0.819
B × C	1	1.57	2.14	0.001206	0.000147	0.000147	0.54	0.73	0.492
Special cubic	1			0.000052	0.000052	0.000052	0.19		0.678
A × B × C	1	1.33	3.04	0.000052	0.000052	0.000052	0.19	0.44	0.678
Residual error	6			0.001640	0.001640	0.000273			
Total	12			0.087665					

near the protonated nitrogen (C7) got deshielded from 161.45 to 164.78 ppm. Also, the intensity of methyl carbon peak (C12) of unreacted MeOH decreased at 48.6 ppm while a new signal (C12') re-labeled to the methyl carbon in MeCO_3^- is observed at 51.45 ppm.

Similar NMR spectra for DBU/MeOH/ CO_2 system are reported by Xie et al. [31] and Cao et al. [39]. Khokarale and Mikkola [67] also used the two-dimensional long range ^1H — ^{13}C HMBC (Hetero-nuclear Multiple Bond Correlation) NMR analysis to investigate the chemical interaction of CO_2 and MeOH molecule. It was observed that during the ionic liquid synthesis, CO_2 reacts to form $[\text{MeOCO}_2^-]$ anion.

The chemical shifts in the ^{13}C NMR spectrum of MEA/DBU/ CO_2 were changed compared to the DBU/MEA mixture (Fig. 9). The carbon close to the protonated nitrogen (C7) was notably shifted downfield

(2.67 ppm). Besides, a new signal for the carbonyl carbon of carbonate anion (C^{***}) was detected at $\delta = 162.76$ ppm which supports the production of $[\text{DBUH}^+][\text{MEACOO}^-]$ as depicted in Path 2 of Fig. 6. The formation of MEA-carbonate anion was also reported by Khokarale et al. [68] using long-range ^1H — ^{13}C HMBC NMR spectroscopy.

3.4.1.2. DBU/MeOH/MEA system. In this study, the three-component DBU/MeOH/MEA CO_2 -BOL was chosen in screening experiments. The ^1H NMR (Fig. 7) and ^{13}C NMR (Fig. 10) spectroscopy were used to characterize the ionic products of CO_2 reaction with solvent. The results were compared with the unreacted mixture of DBU, MEA and MeOH molecules. Fig. 7 illustrates the ^1H NMR spectra of the DBU/MeOH/MEA and the produced ionic liquids ($[\text{DBUH}^+][\text{MEACOO}^-]$ and $[\text{DBUH}^+][\text{CH}_3\text{OCOO}^-]$) based on reaction paths 1 and 2. The broad peak at $\delta = 6.37$ ppm was attributed to the protonation of DBU at nitrogen (N—H) atom on position 6.

The ^{13}C NMR spectra of the MEA/MeOH/ CO_2 (Fig. 10) shows the shifts of characteristic peaks in comparison with to DBU/MeOH/MEA mixture. The signals related to the carbonyl carbons in the anion of the $[\text{DBUH}^+][\text{CH}_3\text{OCOO}^-]$ and $[\text{DBUH}^+][\text{MEACOO}^-]$ were also observed at 158.38 (C^{**}) and 163.28 ppm (C^{***}), respectively.

3.4.1.3. CO_2 absorption in the presence of water. The presence of water as a solvent contaminant has destructive effects on the absorption performance. Spectroscopic studies were performed to evaluate the role of water on the nature of products of CO_2 reaction with BOLs. The effect of MEA was also investigated on the produced ionic species and reaction pathway.

NMR spectroscopic study was performed with wet BOLs (water mole fraction = 0.3) containing DBU/ $\text{H}_2\text{O}/\text{CO}_2$, DBU/MeOH/ $\text{H}_2\text{O}/\text{CO}_2$, DBU/MEA/ $\text{H}_2\text{O}/\text{CO}_2$ and DBU/MeOH/MEA/ $\text{H}_2\text{O}/\text{CO}_2$ systems as well as dried DBU (Figs. 11 and 12).

The ^1H and ^{13}C NMR spectra of dried DBU exhibited no shift in peaks compared to DBU before exposure to CO_2 . Anhydrous DBU does not react with CO_2 in the absence of water [43] such that the solution remains colorless and clear with no solid product precipitation.

The ^1H NMR spectrum of each wet BOL showed a broad singlet (Fig. 11) showing that DBU has been protonated at nitrogen in position 8 (DBU 8'). Also, the bridgehead carbon (C7) shifted downfield compared to unreacted DBU in the ^{13}C NMR spectrum of wet systems (Fig. 12). The ^{13}C NMR spectra also contains new peaks related to the products of CO_2 reaction with BOLs (mole fraction of water = 0.3).

The ^{13}C NMR spectrum in DBU/ $\text{H}_2\text{O}/\text{CO}_2$ system showed that the bridgehead DBU carbon (C7) shifted and a new carboxylate peak was appeared at 162.5 ppm related to bicarbonate anion of the solid product ($[\text{DBUH}^+][\text{HCO}_3^-]$).

The DBU/MeOH/ $\text{H}_2\text{O}/\text{CO}_2$ system also resulted in the production of a white precipitate. The ^{13}C NMR spectrum contains the peaks of bicarbonate (path 5) and methyl carbonate (path 1) salts in 157.4 ppm (*) and 159.7 ppm (**), respectively. The ratio of equilibrium constants of

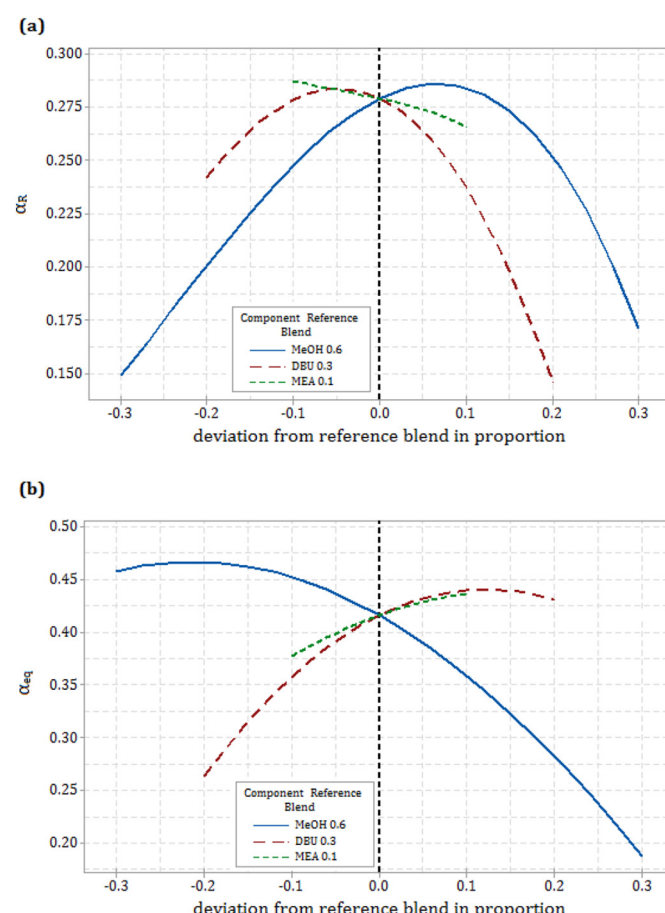


Fig. 5. Cox response trace plots for the effect of component proportions on the (a) α_R and (b) α_{eq} in the DBU/MEA/MeOH BOL at the temperature of 308.2 K and the initial CO_2 pressure of 25.00 bar.

reaction 5 (path 5) and **reaction 1** (path 1) based on Fig. 6 was calculated to be 1.43 from the NMR integration ratio by bubbling CO₂ through 1:1:1 mixture of MeOH, water and DBU [34]. The K_{H2O}/K_{MeOH} value shows that DBU reacts more favorably with water rather than MeOH in a competitive binding experiment. The results suggest that H₂O, as a shorter and more acidic molecule than MeOH, binds more strongly such that any water in the reaction medium would be in direct competition with alcohols.

Addition of MEA to DBU/H₂O mixture led to the formation of [DBUH⁺][MEACOO⁻] salt (Fig. 6, path 2). Therefore, a new peak appeared at 163.7 ppm in ¹³C NMR spectrum (C***). The resultant product was a viscous liquid without solid precipitation. The formation of bicarbonate salt was inhibited due to the addition of MEA to the mixture. Cieslarova et al. [69] proposed that protonated or non-protonated MEA (depending on the solution pH) have an alcohol group prone to react with HCO₃⁻ (Fig. 6, path7) to produce a carbonate salt. Moreover, free MEA and its carbamate are available in certain amounts of CO₂ loading that react with HCO₃⁻ based on path 6 of Fig. 6. The equilibrium constant of MEA carbonate formation was calculated to be 0.66 based on the initial concentrations and peak areas in the NMR spectra [69]. The bicarbonate salt formation was also inhibited by the addition of MEA to the DBU/MeOH/H₂O mixture prior to reaction with CO₂. A new signal related to the carbonyl carbon (C****) of MEA-carbonate salt appeared in the ¹³C NMR spectrum of DBU/MeOH/H₂O/CO₂.

3.4.2. FTIR spectroscopy

The FTIR spectra of DBU, DBU/H₂O/CO₂, DBU/MeOH, and DBU/MeOH/CO₂, DBU/MEA, DBU/MEA/CO₂, DBU/MeOH/MEA and DBU/MeOH/MEA/CO₂ systems are compared in Fig. 13 to characterize the functional groups in ionic products.

The spectrum of mixtures containing MeOH depicts an absorption peak at 1046 cm⁻¹ related to the C—O vibration of MeOH. The observed peak at 1614 cm⁻¹, belongs to the C = N ring stretching vibration in all the unreacted solvents. This peak becomes weaker and shifts to 1588 cm⁻¹ after the CO₂ absorption. Moreover, a strong absorption also appeared at 1648 cm⁻¹ that relates to C=O stretching absorption band. The C—H stretching vibrations were also observed at 2929 cm⁻¹ and 2842 cm⁻¹ in the ring of DBU, MeOH and MEA which also observed even after reaction. The N—H stretching at 3099 cm⁻¹ and 3242 cm⁻¹ supports the protonation of the DBU after CO₂ absorption in the BOLs.

3.4.3. Equilibrium CO₂ absorption

The equilibrium solubility data for the absorption of CO₂ in DBU/MeOH (1/2) and DBU/MeOH/MEA (0.3/0.6/0.1) CO₂-BOLs were measured in the temperatures of 308.2 and 318.2 K and pressure range of 0–33 bar. The results are presented in Fig. 14. Addition of MEA to the DBU/MeOH BOL, while keeping the molar ratio fixed at 1/2, results in the higher CO₂ uptake. The positive effect of MEA on the equilibrium CO₂ absorption was also observed in Fig. 5. Increasing the temperature from 35 °C to 45 °C in both CO₂-BOLs (DBU/MeOH and DBU/MeOH/MEA) shifts the equilibrium and

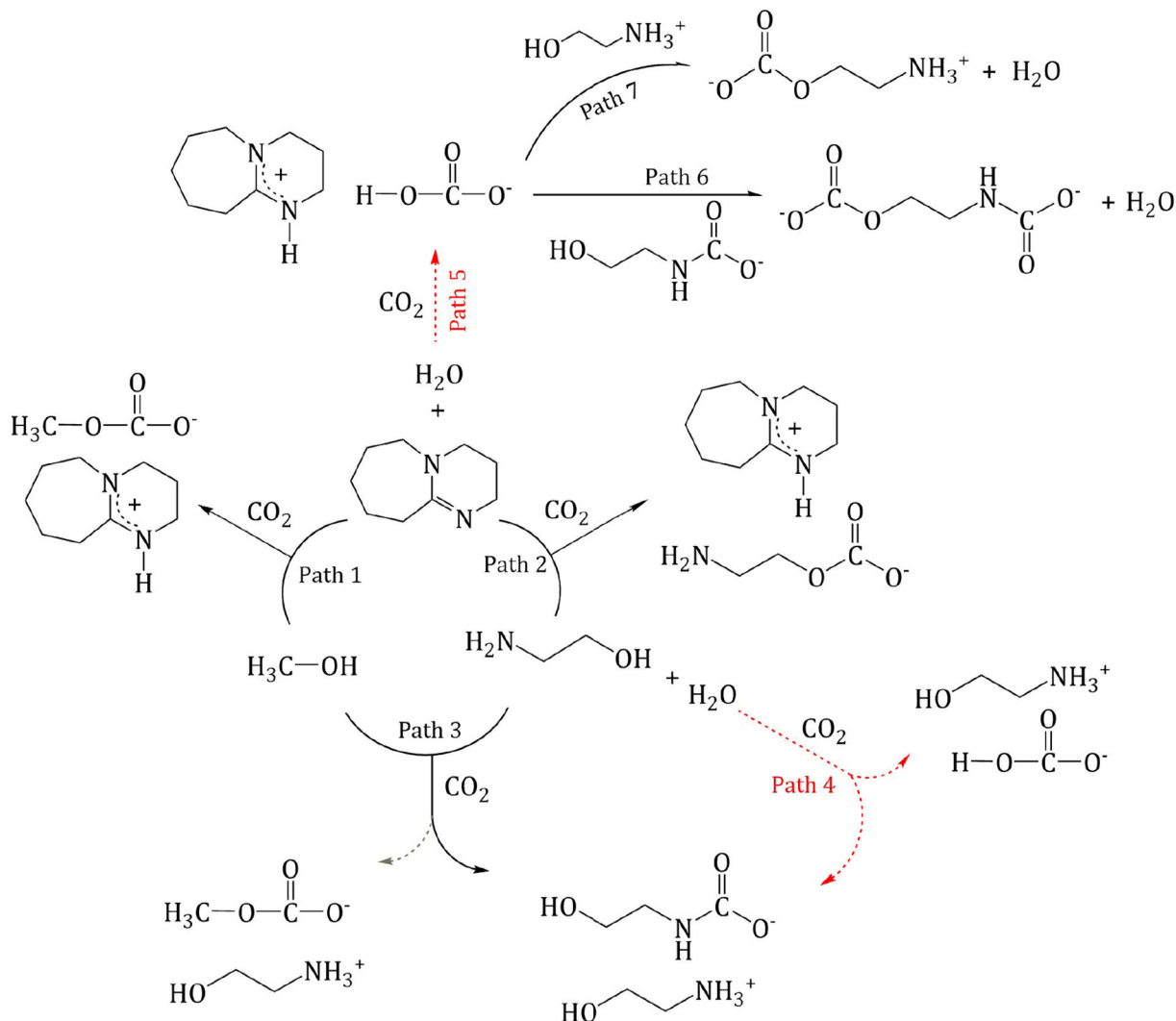


Fig. 6. Plausible reaction mechanism for the absorption of CO₂ in the MEA modified DBU/MeOH BOL in the presence of water.

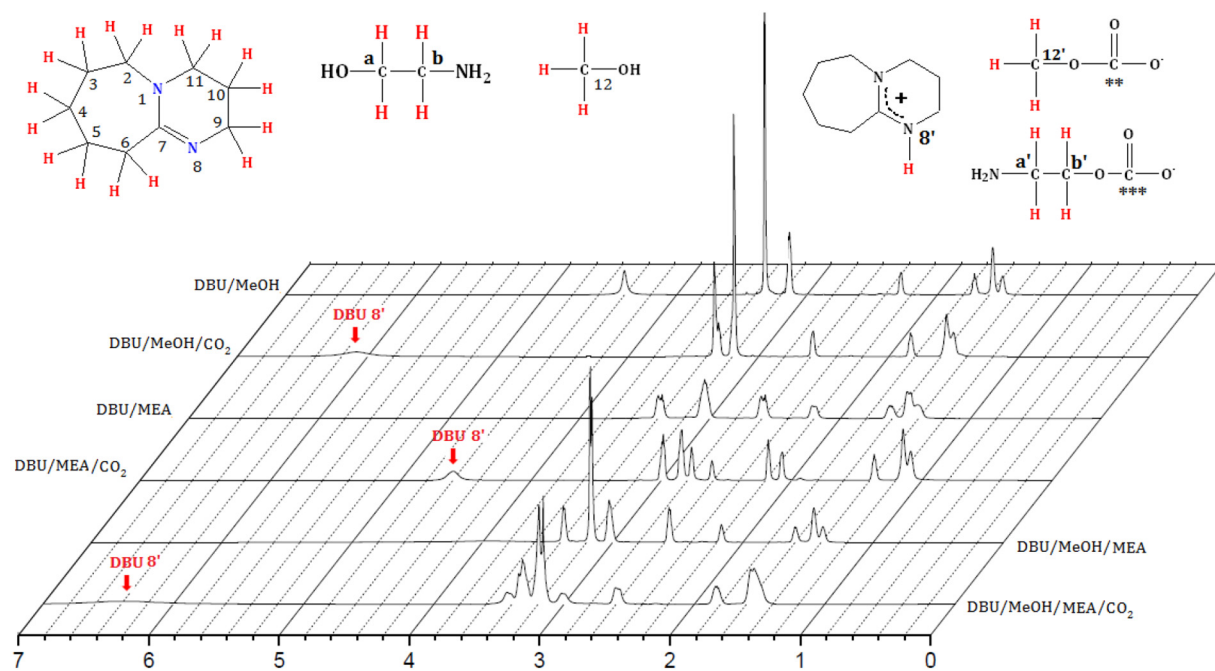


Fig. 7. ^1H NMR spectra for the DBU/MeOH, DBU/MeOH/ CO_2 , DBU/MEA, DBU/MEA/ CO_2 , DBU/MeOH/MEA and DBU/MeOH/MEA/ CO_2 mixtures in CDCl_3 ($\delta = 7.28$ ppm).

results in the lower CO_2 solubility. The CO_2 solubility in the BOLs is directly proportional to the CO_2 pressure.

4. Conclusions

The DBU/MeOH/MEA BOL with the molar ratio of 0.3/0.53/0.17 was selected in the screening experiments and in mixture design approach

based on the CO_2 absorption rate and capacity. It was observed that the addition of MEA as a promoter to the two-component BOL comprised of DBU and MeOH leads to the higher CO_2 absorption capacity. Spectroscopic studies of the reaction between DBU, MEA, MeOH and CO_2 in the presence and absence of water was also done with the aim of clarifying the role of MEA and the nature of the isolated products. Addition of MEA to the two-component BOLs resulted in the inhibition of

Table 6

^1H NMR chemical shifts of relevant species in the spectra of DBU/MEA, DBU/MEA/ CO_2 , DBU/MeOH and DBU/MeOH/ CO_2 mixtures in CDCl_3 ($\delta = 7.28$ ppm).

DBU/MEA	DBU/MEA/ CO_2			DBU/MeOH			DBU/MeOH/ CO_2					
	^1H atom (before reaction)	nH	δ	^1H atom (after reaction)	nH	δ	^1H atom (before reaction)	nH	δ	^1H atom (after reaction)	nH	δ
DBU (3–5)	6	1.40	DBU (3', 4', 5')	6	1.08	DBU (3–5)	6	1.49	DBU (3', 4', 5')	6	1.50	
DBU (10)	2	1.47	DBU (10')	2	1.14	DBU (10)	2	1.57	DBU (10')	2	1.55	
DBU (6)	2	1.60	DBU (6')	2	1.36	DBU (6)	2	1.71	DBU (6')	2	1.83	
DBU (9)	2	2.19	DBU (9')	2	2.07–2.18	DBU (9)	2	2.28	DBU (9')	2	2.57	
DBU (2, 11)	4	3.03	DBU (2', 11')	4	2.76–2.84	DBU (2, 11)	4	3.13–3.14	DBU (2', 11')	4	3.30–3.34	
MEA-b	2	2.58	MEA-b'	2	2.61	CH_3OH (1)	3	3.32	CH_3OH (1)	3	3.19	
MEA-a	2	3.37	MEA-a'	2	2.98	$\overline{\text{CH}_3\text{OH}}$ (2)	1	4.40	$\overline{\text{CH}_3\text{OH}}$ (2)	1	4.30	
		DBU (8')		1	4.59				DBU (8)		1	6.08

Table 7

^{13}C NMR shifts and signal assignments in spectra of DBU/MEA and DBU/MEA/ CO_2 . Shifts are referred to an internal standard, CDCl_3 ($\delta = 76.3$).

DBU/MEA		DBU/MEA/ CO_2		DBU/MeOH		DBU/MeOH/ CO_2	
^{13}C atom (before reaction)	δ	^{13}C atom (after reaction)	δ	^{13}C atom (before reaction)	δ	^{13}C atom (after reaction)	δ
DBU (10)	21.10	DBU (10)	19.18	DBU (10)	21.02	DBU (10)	18.48
DBU (4)	24.64	DBU (4)	23.31	DBU (4)	24.59	DBU (4)	22.88
DBU (5)	27.21	DBU (5)	25.95	DBU (5)	27.21	DBU (5)	25.65
DBU (3)	28.48	DBU (3)	27.76	DBU (3)	28.52	DBU (3)	27.84
DBU (6)	35.34	DBU (6)	32.26	DBU (6)	35.01	DBU (6)	31.08
DBU (9)	42.96	DBU (9)	42.76	DBU (9)	42.09	DBU (9)	37.13
DBU (11)	47.14	DBU (11)	46.91	DBU (11)	47.21	DBU (11)	47.38
DBU (2)	51.65	DBU (2)	52.03	DBU (2)	51.76	DBU (2)	53.01
DBU (7)	160.91	DBU (7)	163.85	DBU (7)	161.45	DBU (7)	164.78
MEA-a	62.11	MEA-b	61.75	CH_3OH	48.68	CH_3OH	48.63
MEA-b	42.36	MEA-a	38.75			CH_3OCOO^- (1)	51.45
		$\overline{\text{MEACOO}}^-$	162.76			$\overline{\text{CH}_3\text{OCOO}}^-$ (2)	158.34

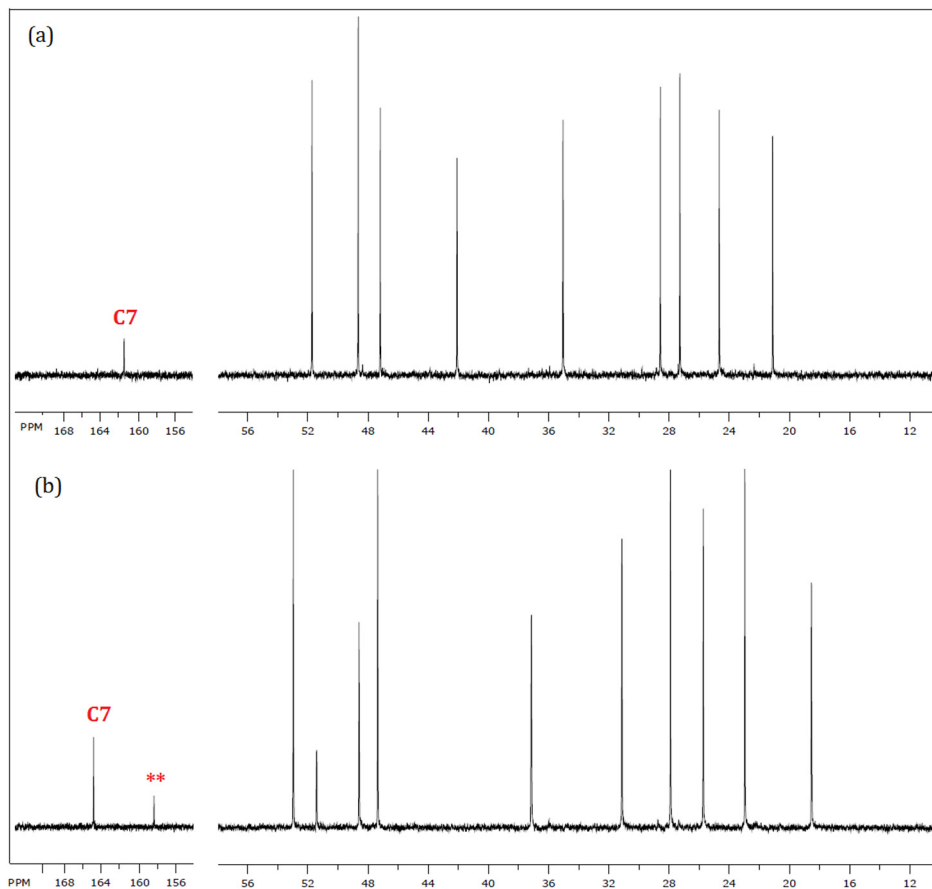


Fig. 8. ^{13}C NMR spectra of (a) DBU/MeOH and (b) DBU/MeOH/CO₂ ($[\text{DBUH}^+][\text{MeOOCO}^-]$).

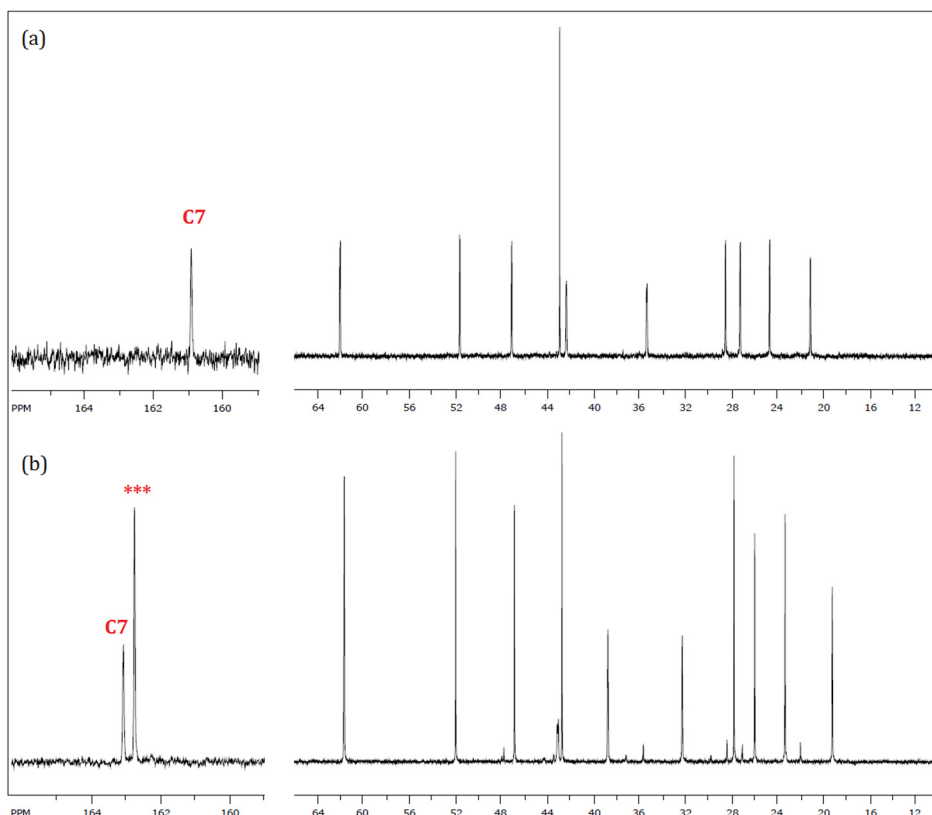


Fig. 9. ^{13}C NMR spectra of (a) DBU/MEA and (b) DBU/MEA/CO₂ ($[\text{DBUH}^+][\text{MEACOO}^-]$).

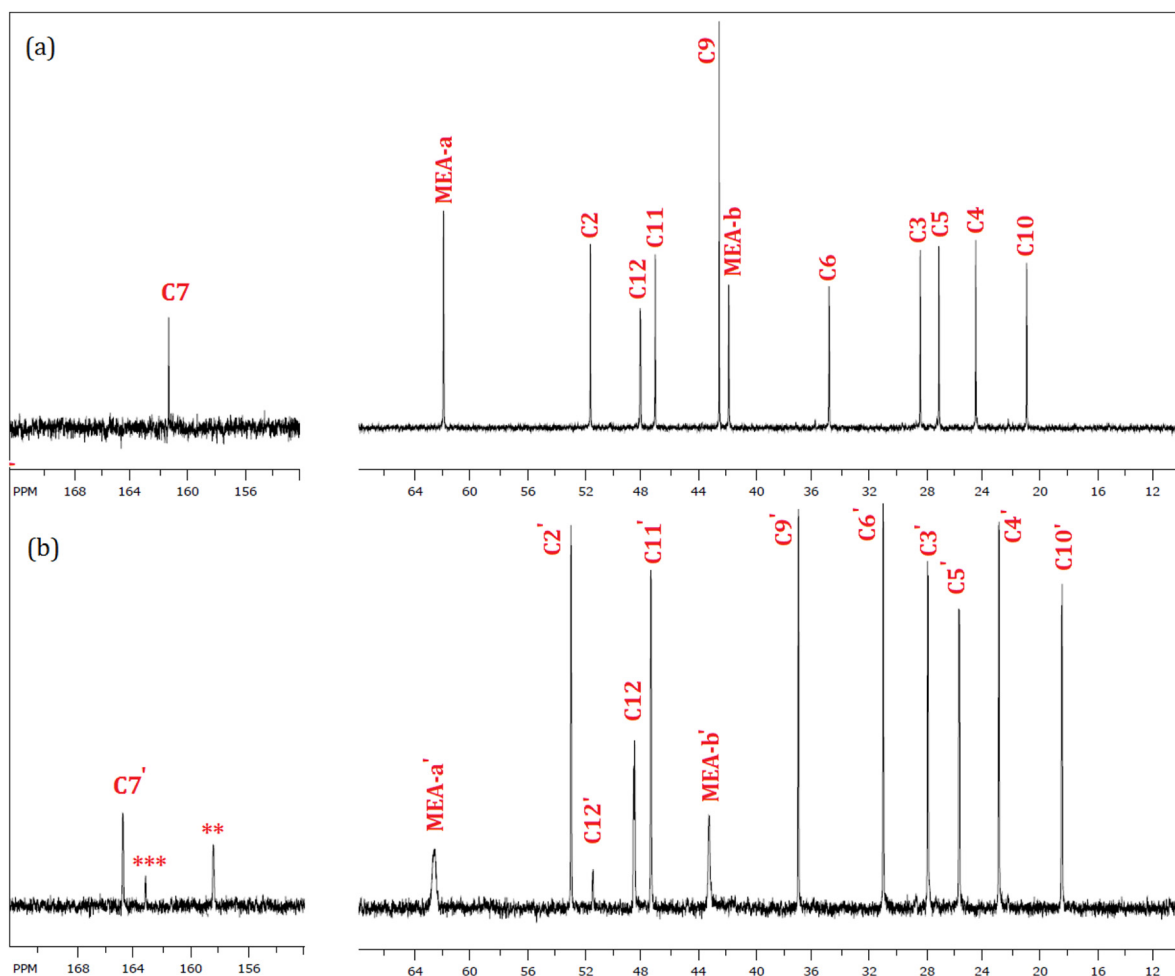


Fig. 10. ¹³C NMR spectra of (a) DBU/MeOH/MEA and (b) DBU/MeOH/MEA/CO₂ systems.

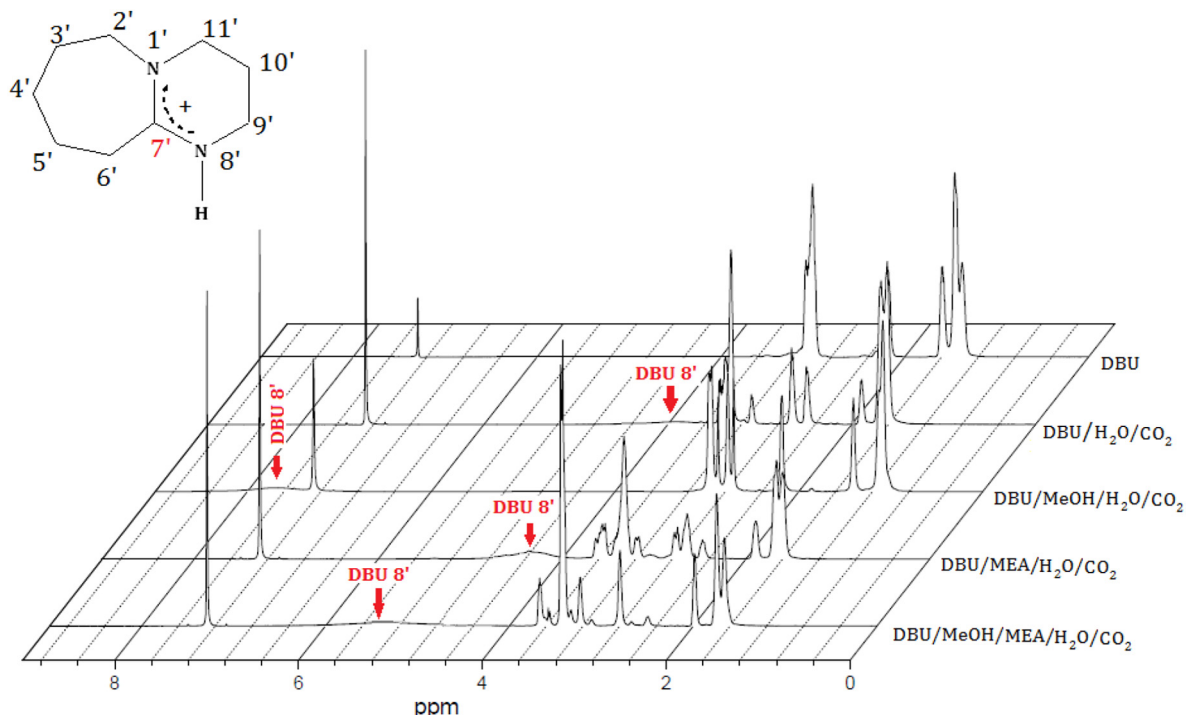


Fig. 11. ¹H NMR spectra of DBU/CO₂, DBU/H₂O/CO₂, DBU/MeOH/H₂O/CO₂, DBU/MEA/H₂O/CO₂ and DBU/MeOH/MEA/H₂O/CO₂ systems in CDCl₃ ($\delta = 7.28$ ppm).

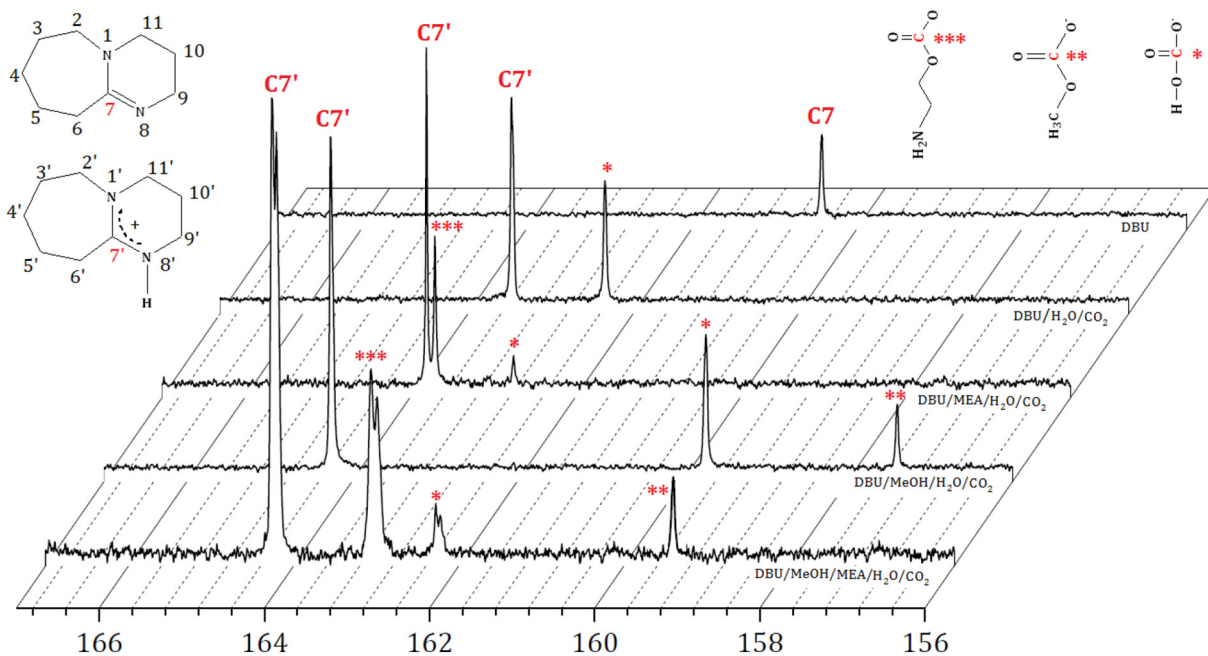


Fig. 12. ^{13}C NMR spectra DBU/ CO_2 , DBU/ $\text{H}_2\text{O}/\text{CO}_2$, DBU/ $\text{MeOH}/\text{H}_2\text{O}/\text{CO}_2$, DBU/ $\text{MEA}/\text{H}_2\text{O}/\text{CO}_2$ and DBU/ $\text{MeOH}/\text{MEA}/\text{H}_2\text{O}/\text{CO}_2$ systems.

solid bicarbonate salt precipitation. The production of alkyl carbonate salts rather than carbamate salt, using the proposed BOL (DBU/MeOH/MEA) for CO_2 capture, is advantageous because lower regeneration

energy is needed for solvent recovery. Therefore, the introduced green solvents in this study can be used for energy efficient CO_2 absorption with no need for scrupulously dry conditions.

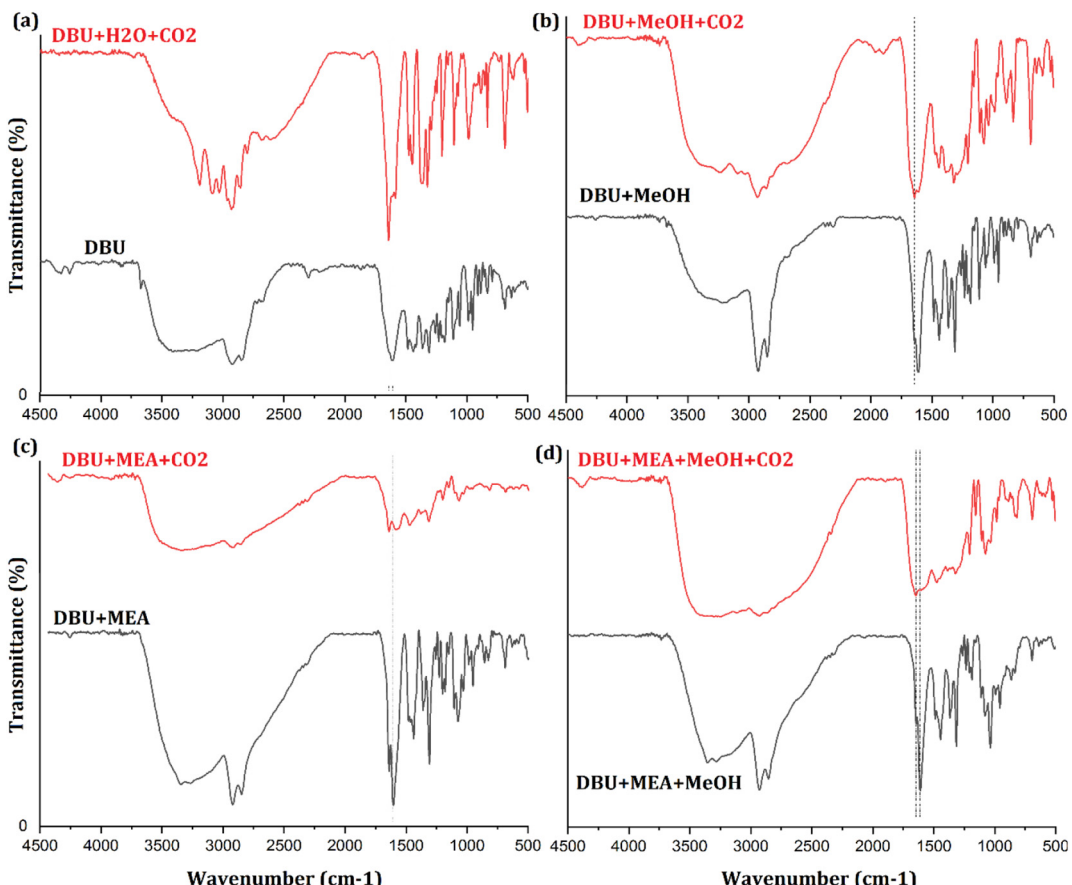


Fig. 13. FTIR spectrum of (a) DBU and DBU/ $\text{H}_2\text{O}/\text{CO}_2$ (b) DBU/ MeOH and DBU/ MeOH/CO_2 (c) DBU/ MEA and DBU/ MEA/CO_2 (d) DBU/ MEA/MeOH and DBU/ $\text{MEA}/\text{MeOH}/\text{CO}_2$ systems.

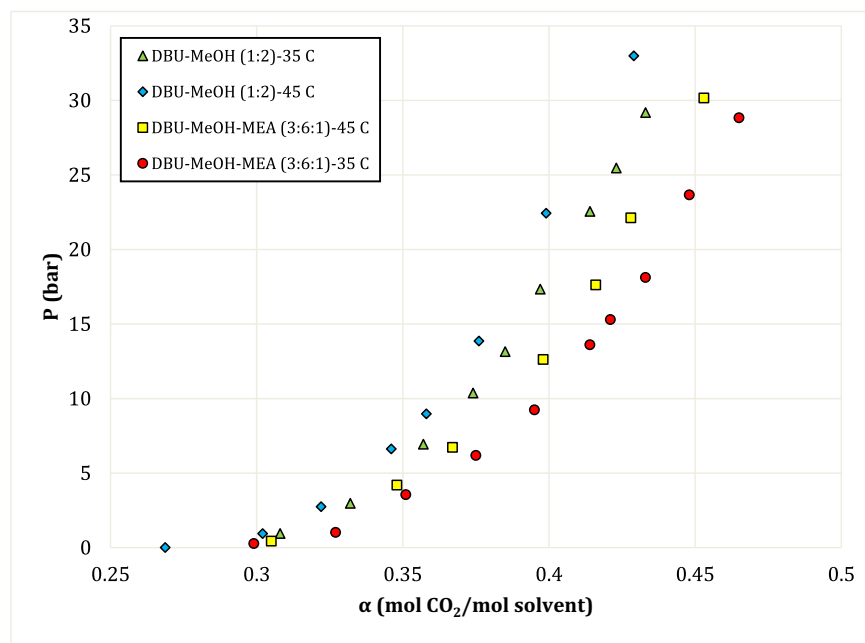


Fig. 14. The equilibrium solubility of CO₂ in DBU/MeOH (1/2) and DBU/MeOH/MEA (0.3/0.6/0.1) mixtures in the pressure range of 0–33 bar and the temperatures of 308.2 and 318.2 K.

CRediT authorship contribution statement

Ali Hedayati: Conceptualization, Methodology, Validation, Formal analysis, Investigation, Writing - original draft, Visualization. **Farzaneh Feyzi:** Resources, Writing - review & editing, Supervision, Project administration, Funding acquisition, Visualization.

Declaration of competing interest

The authors declare that they have no known competing financial interests or personal relationships that could have appeared to influence the work reported in this paper.

Acknowledgments

The financial support provided by Iran National Science Foundation (grant number: 97011809) is gratefully acknowledged.

References

- [1] F. Liu, G. Jing, B. Lv, Z. Zhou, High regeneration efficiency and low viscosity of CO₂ capture in a switchable ionic liquid activated by 2-amino-2-methyl-1-propanol, International Journal of Greenhouse Gas Control 60 (2017) 162–171.
- [2] M. Raji, A. Dashti, P. Amani, A.H. Mohammadi, Efficient estimation of CO₂ solubility in aqueous salt solutions, J. Mol. Liq. 283 (2019) 804–815.
- [3] P.M. Matthias, F. Zheng, D.J. Heldebrant, A. Zwoster, G. Whyatt, C.M. Freeman, P. Koech, Measuring the absorption rate of CO₂ in nonaqueous CO₂-binding organic liquid solvents with a wetted-wall apparatus, ChemSusChem 8 (21) (2015) 3617–3625.
- [4] M. Raji, A. Dashti, P. Amani, A.H. Mohammadi, Efficient estimation of CO₂ solubility in aqueous salt solutions, J. Mol. Liq. 283 (2019) 804–815.
- [5] G.V. Carrera, M.N. da Ponte, L.C. Branco, Synthesis and properties of reversible ionic liquids using CO₂, mono-to multiple functionalization, Tetrahedron 68 (36) (2012) 7408–7413.
- [6] M.C. Ozturk, O.Y. Orhan, E. Alper, Kinetics of carbon dioxide binding by 1, 1, 3, 3-tetramethylguanidine in 1-hexanol, International Journal of Greenhouse Gas Control 26 (2014) 76–82.
- [7] S. Delavari, N.A.S. Amin, Photocatalytic conversion of CO₂ and CH₄ over immobilized titania nanoparticles coated on mesh: optimization and kinetic study, Appl. Energy 162 (2016) 1171–1185.
- [8] M.R. Mahi, I. Mokbel, L. Negadi, F. Dergal, J. Jose, Experimental solubility of carbon dioxide in monoethanolamine, diethanolamine or N-methyldiethanolamine (30 wt%) dissolved in deep eutectic solvent (choline chloride and ethylene glycol solution), J. Mol. Liq. 289 (2019), 111062.
- [9] E. Privalova, M. Nurmi, M.S. Maraño, E.V. Murzina, P. Mäki-Arvela, K. Eränen, ... J.P. Mikkola, CO₂ removal with 'switchable' versus 'classical' ionic liquids, Separation and purification technology 97 (2012) 42–50.
- [10] D. Camper, J.E. Bara, D.L. Gin, R.D. Noble, Room-temperature ionic liquid-amine solutions: tunable solvents for efficient and reversible capture of CO₂, Ind. Eng. Chem. Res. 47 (21) (2008) 8496–8498.
- [11] Carrera, G. V. S. M., Jordão, N., Branco, L. C., & da Ponte, M. N. (2015). CO₂ capture systems based on saccharides and organic superbases. Faraday Discuss., 183, 429–444.
- [12] S. Kumar, J.H. Cho, I.L. Moon, Ionic liquid-amine blends and CO₂BOLs: prospective solvents for natural gas sweetening and CO₂ capture technology—a review, International Journal of Greenhouse Gas Control 20 (2014) 87–116.
- [13] Q. Zhuang, B. Clements, CO₂ capture by biphasic absorbent-absorption performance and VLE characteristics, Energy 147 (2018) 169–176.
- [14] Y.E. Kim, J.H. Park, S.H. Yun, S.C. Nam, S.K. Jeong, Y.I. Yoon, Carbon dioxide absorption using a phase transitional alkanolamine-alcohol mixture, J. Ind. Eng. Chem. 20 (4) (2014) 1486–1492.
- [15] F. Barzaghi, C. Giorgi, F. Mani, M. Peruzzini, Reversible carbon dioxide capture by aqueous and non-aqueous amine-based absorbents: a comparative analysis carried out by ¹³C NMR spectroscopy, Appl. Energy 220 (2018) 208–219.
- [16] M.K. Kang, S.B. Jeon, J.H. Cho, J.S. Kim, K.J. Oh, Characterization and comparison of the CO₂ absorption performance into aqueous, quasi-aqueous and non-aqueous MEA solutions, International Journal of Greenhouse Gas Control 63 (2017) 281–288.
- [17] Y.S. Yu, H.F. Lu, T.T. Zhang, Z.X. Zhang, G.X. Wang, V. Rudolph, Determining the performance of an efficient nonaqueous CO₂ capture process at desorption temperatures below 373 K, Ind. Eng. Chem. Res. 52 (35) (2013) 12622–12634.
- [18] C. Guo, S. Chen, Y. Zhang, G. Wang, Solubility of CO₂ in nonaqueous absorption system of 2-(2-aminoethylamine) ethanol + benzyl alcohol, J. Chem. Eng. Data 59 (6) (2014) 1796–1801.
- [19] F. Barzaghi, S. Lai, F. Mani, Novel non-aqueous amine solvents for reversible CO₂ capture, Energy Procedia 63 (2014) 1795–1804.
- [20] F. Barzaghi, F. Mani, M. Peruzzini, Efficient CO₂ absorption and low temperature de-sorption with non-aqueous solvents based on 2-amino-2-methyl-1-propanol (AMP), International Journal of Greenhouse Gas Control 16 (2013) 217–223.
- [21] V. Barbarossa, F. Barzaghi, F. Mani, S. Lai, P. Stoppioni, G. Vanga, Efficient CO₂ capture by non-aqueous 2-amino-2-methyl-1-propanol (AMP) and low temperature solvent regeneration, RSC Adv. 3 (30) (2013) 12349–12355.
- [22] S.W. Park, B.S. Choi, J.W. Lee, Chemical absorption of carbon dioxide with triethanolamine in non-aqueous solutions, Korean J. Chem. Eng. 23 (1) (2006) 138–143.
- [23] G.F. Versteeg, W.P.M. van Swaaij, On the kinetics between CO₂ and alkanolamines both in aqueous and non-aqueous solutions—II. Tertiary amines, Chem. Eng. Sci. 43 (3) (1988) 587–591.
- [24] G.F. Versteeg, W.P.M. van Swaaij, On the kinetics between CO₂ and alkanolamines both in aqueous and non-aqueous solutions—I. Primary and secondary amines, Chem. Eng. Sci. 43 (3) (1988) 573–585.
- [25] S. Kang, Y.G. Chung, J.H. Kang, H. Song, CO₂ absorption characteristics of amino group functionalized imidazolium-based amino acid ionic liquids, J. Mol. Liq. (2019) 111825.
- [26] S. Sardar, A. Mumtaz, M. Yasinzai, C.D. Wilfred, Synthesis, thermophysical properties and CO₂ sorption of imidazolium, thiazolium, iminium and morpholinium-based

- protic ionic liquids paired with 2-acrylamido-2-methyl-1-propanesulfonate anion, *J. Mol. Liq.* (2019) 111843.
- [27] I. Anugwom, P. Mäki-Arvela, P. Virtanen, P. Damlin, R. Sjöholm, J.P. Mikkola, Switchable ionic liquids (SILs) based on glycerol and acid gases, *RSC Adv.* 1 (3) (2011) 452–457.
- [28] G. Laus, G. Bentivoglio, H. Schottenberger, V. Kahlenberg, H. Kopacka, T. Röder, H. Sixta, Ionic liquids: current developments, potential and drawbacks for industrial applications, *Lenzinger Berichte* 84 (2005) 71–85.
- [29] M.C. Özürk, C.S. Ume, E. Alper, Reaction mechanism and kinetics of 1, 8-diazabicyclo [5.4.0] undec-7-ene and carbon dioxide in alkanol solutions, *Chemical Engineering & Technology* 35 (12) (2012) 2093–2098.
- [30] P.G. Jessop, D.J. Heldebrant, X. Li, C.A. Eckert, C.L. Liotta, Green chemistry: reversible nonpolar-to-polar solvent, *Nature* 436 (7054) (2005) 1102.
- [31] Y. Xie, R. Parnas, B. Liang, Y. Liu, C. Tao, H. Lu, Synthesis and characterization of switchable ionic compound based on DBU, CH₃OH, and CO₂, *Chin. J. Chem. Eng.* 23 (10) (2015) 1728–1732.
- [32] C.J. Clarke, W.C. Tu, O. Levers, A. Bröhl, J.P. Hallett, Green and sustainable solvents in chemical processes, *Chem. Rev.* 118 (2) (2018) 747–800.
- [33] P. Pollet, E.A. Davey, E.E. Ureña-Benavides, C.A. Eckert, C.L. Liotta, Solvents for sustainable chemical processes, *Green Chem.* 16 (3) (2014) 1034–1055.
- [34] D.J. Heldebrant, C.R. Yonker, P.G. Jessop, L. Phan, Organic liquid CO₂ capture agents with high gravimetric CO₂ capacity, *Energy Environ. Sci.* 1 (4) (2008) 487–493.
- [35] J.R. Switzer, A.L. Ethier, K.M. Flack, E.J. Biddinger, L. Gelbaum, P. Pollet, C.L. Liotta, Reversible ionic liquid stabilized carbamic acids: a pathway toward enhanced CO₂ capture, *Ind. Eng. Chem. Res.* 52 (36) (2013) 13159–13163.
- [36] Y. Wang, Q. Han, H. Wen, Theoretical discussion on the mechanism of binding CO₂ by DBU and alcohol, *Mol. Simul.* 39 (10) (2013) 822–827.
- [37] M. Gonzalez-Miquel, M. Talreja, A.L. Ethier, K. Flack, J.R. Switzer, E.J. Biddinger, C.L. Liotta, COSMO-RS studies: structure–property relationships for CO₂ capture by reversible ionic liquids, *Ind. Eng. Chem. Res.* 51 (49) (2012) 16066–16073.
- [38] C. Wang, S.M. Mahurin, H. Luo, G.A. Baker, H. Li, S. Dai, Reversible and robust CO₂ capture by equimolar task-specific ionic liquid–superbase mixtures, *Green Chem.* 12 (5) (2010) 870–874.
- [39] X. Cao, H. Xie, Z. Wu, H. Shen, B. Jing, Phase-switching homogeneous catalysis for clean production of biodiesel and glycerol from soybean and microbial lipids, *ChemCatChem* 4 (9) (2012) 1272–1278.
- [40] M.C. Özürk, C.S. Ume, E. Alper, Reaction mechanism and kinetics of 1, 8-diazabicyclo [5.4.0] undec-7-ene and carbon dioxide in alkanol solutions, *Chemical Engineering & Technology* 35 (12) (2012) 2093–2098.
- [41] G.A. Whyatt, C.J. Freeman, A. Zwoster, D.J. Heldebrant, Measuring nitrous oxide mass transfer into non-aqueous CO₂BOL CO₂ capture solvents, *Ind. Eng. Chem. Res.* 55 (16) (2016) 4720–4725.
- [42] A. Ostonen, E. Sapei, P. Uusi-Kyyny, A. Klemelä, V. Alopaeus, Measurements and modeling of CO₂ solubility in 1, 8-diazabicyclo-[5.4.0]-undec-7-ene-glycerol solutions, *Fluid Phase Equilib.* 374 (2014) 25–36.
- [43] D.J. Heldebrant, P.G. Jessop, C.A. Thomas, C.A. Eckert, C.L. Liotta, The reaction of 1, 8-diazabicyclo [5.4.0] undec-7-ene (DBU) with carbon dioxide, *The Journal of Organic Chemistry* 70 (13) (2005) 5335–5338.
- [44] T. Yamada, P.J. Lukac, T. Yu, R.G. Weiss, Reversible, room-temperature, chiral ionic liquids. Amidinium carbamates derived from amidines and amino-acid esters with carbon dioxide, *Chem. Mater.* 19 (19) (2007) 4761–4768.
- [45] T. Yamada, P.J. Lukac, M. George, R.G. Weiss, Reversible, room-temperature ionic liquids. Amidinium carbamates derived from amidines and aliphatic primary amines with carbon dioxide, *Chem. Mater.* 19 (5) (2007) 967–969.
- [46] T. Yu, T. Yamada, G.C. Gaviola, R.G. Weiss, Carbon dioxide and molecular nitrogen as switches between ionic and uncharged room-temperature liquids comprised of amidines and chiral amino alcohols, *Chem. Mater.* 20 (16) (2008) 5337–5344.
- [47] M.K. Park, O.C. Sandall, Solubility of carbon dioxide and nitrous oxide in 50 mass methyl diethanolamine, *J. Chem. Eng. Data* 46 (1) (2001) 166–168.
- [48] A.T. Zoghi, F. Feyzi, S. Zarrinpashneh, Experimental investigation on the effect of addition of amine activators to aqueous solutions of N-methyldiethanolamine on the rate of carbon dioxide absorption, *International Journal of Greenhouse Gas Control* 7 (2012) 12–19.
- [49] A. Najafloo, A.T. Zoghi, F. Feyzi, Measuring solubility of carbon dioxide in aqueous blends of N-methyldiethanolamine and 2-((2-aminoethyl) amino) ethanol at low CO₂ loadings and modelling by electrolyte SAFT-HR EoS, *J. Chem. Thermodyn.* 82 (2015) 143–155.
- [50] A.T. Zoghi, F. Feyzi, S. Zarrinpashneh, Equilibrium solubility of carbon dioxide in a 30wt.% aqueous solution of 2-((2-aminoethyl) amino) ethanol at pressures between atmospheric and 4400kPa: an experimental and modelling study, *J. Chem. Thermodyn.* 44 (1) (2012) 66–74.
- [51] D.Y. Peng, D.B. Robinson, A new two-constant equation of state, *Industrial & Engineering Chemistry Fundamentals* 15 (1) (1976) 59–64.
- [52] M. Wagner, I. von Harbou, J. Kim, I. Ermatchkova, G. Maurer, H. Hasse, Solubility of carbon dioxide in aqueous solutions of monoethanolamine in the low and high gas loading regions, *J. Chem. Eng. Data* 58 (4) (2013) 883–895.
- [53] V. Zeleňák, M. Skřínska, A. Zukal, J. Čejka, Carbon dioxide adsorption over amine modified silica: effect of amine basicity and entropy factor on isoteric heats of adsorption, *Chem. Eng. J.* 348 (2018) 327–337.
- [54] V. Zelenak, D. Halamova, L. Gabrova, E. Bloch, P. Llewellyn, Amine-modified SBA-12 mesoporous silica for carbon dioxide capture: effect of amine basicity on sorption properties, *Microporous Mesoporous Mater.* 116 (1–3) (2008) 358–364.
- [55] K.R. Putta, H.F. Svendsen, H.K. Knuttila, CO₂ absorption into loaded aqueous MEA solutions: impact of different model parameter correlations and thermodynamic models on the absorption rate model predictions, *Chem. Eng. J.* 327 (2017) 868–880.
- [56] S. Sardar, A. Mumtaz, M. Yasinza, C.D. Wilfred, Synthesis, thermophysical properties and CO₂ sorption of imidazolium, thiazolium, iminium and morpholinium-based protic ionic liquids paired with 2-acrylamido-2-methyl-1-propanesulfonate anion, *J. Mol. Liq.* (2019) 111843.
- [57] E. Sada, H. Kumazawa, Y. Osawa, M. Matsuura, Z.Q. Han, Reaction kinetics of carbon dioxide with amines in non-aqueous solvents, *The Chemical Engineering Journal* 33 (2) (1986) 87–95.
- [58] L. Phan, D. Chiu, D.J. Heldebrant, H. Huttenhower, E. John, X. Li, P.G. Jessop, Switchable solvents consisting of amidine/alcohol or guanidine/alcohol mixtures, *Ind. Eng. Chem. Res.* 47 (3) (2008) 539–545.
- [59] V.M. Blasucci, R. Hart, P. Pollet, C.L. Liotta, C.A. Eckert, Reversible ionic liquids designed for facile separations, *Fluid Phase Equilib.* 294 (1–2) (2010) 1–6.
- [60] S. Thanitwatthanasa, L.M. Sagis, P. Chitprasert, Pluronic F127/Pluronic P123/vitamin E TPGS mixed micelles for oral delivery of mangiferin and quercetin: mixture-design optimization, micellization, and solubilization behavior, *J. Mol. Liq.* 274 (2019) 223–238.
- [61] M.A. Bezerra, V.A. Lemos, C.G. Novaes, R.M. de Jesus, H.R. Souza Filho, S.A. Araújo, J.P.S. Alves, Application of mixture design in analytical chemistry, *Microchem. J.* (2019) 104336.
- [62] N.S. Nouadje, E. Nso, E.G. Kana, C. Kapseu, Simplex lattice mixture design application for biodiesel production: formulation and characterization of hybrid oil as feedstock, *Fuel* 252 (2019) 135–142.
- [63] C. Chen, X. Li, X. Chen, J. Chai, H. Tian, Development of cemented paste backfill based on the addition of three mineral additions using the mixture design modeling approach, *Constr. Build. Mater.* 229 (2019), 116919.
- [64] A.M. Vohra, C.V. Patel, P. Kumar, H.P. Thakkar, Development of dual drug loaded solid self microemulsifying drug delivery system: exploring interfacial interactions using QbD coupled risk based approach, *J. Mol. Liq.* 242 (2017) 1156–1168.
- [65] A.H. Rad, H.R. Pirouzian, O.S. Toker, N. Konar, Application of simplex lattice mixture design for optimization of sucrose-free milk chocolate produced in a ball mill, *LWT* 115 (2019) 108435.
- [66] A.C. Dias, M.P.F. Fontes, C. Reis, C.R. Bellato, S. Fendorf, Simplex-centroid mixture design applied to arsenic (V) removal from waters using synthetic minerals, *J. Environ. Manag.* 238 (2019) 92–101.
- [67] S.G. Khokarale, J.P. Mikkola, Efficient and catalyst free synthesis of acrylic plastic precursors: methyl propionate and methyl methacrylate synthesis through reversible CO₂ capture, *Green Chem.* 21 (8) (2019) 2138–2147.
- [68] S.G. Khokarale, T. Le-That, J.P. Mikkola, Carbohydrate free lignin: a dissolution-recovery cycle of sodium lignosulfonate in a switchable ionic liquid system, *ACS Sustain. Chem. Eng.* 4 (12) (2016) 7032–7040.
- [69] Z. Cieslarova, V.B. dos Santos, C.L. do Lago, Both carbamates and monoalkyl carbonates are involved in carbon dioxide capture by alkanolamines, *International Journal of Greenhouse Gas Control* 76 (2018) 142–149.